Inhibition of the glucocorticoid-activating enzyme 11β-hydroxysteroid dehydrogenase type 1 drives concurrent 11-oxygenated androgen excess

Lina Schiffer[1,#], Imken Oestlund[2,#], Jacky Snoep[2,3], Lorna C. Gilligan[1], Angela E. Taylor[1], Alexandra J. Sinclair[1], Rishi Singhal[4], Adrian Freeman[5], Ramzi Ajjan[6,7], Ana Tiganescu[6,7], Wiebke Arlt[1,8,9] and Karl-Heinz Storbeck[1,2]

[1] Institute of Metabolism and Systems Research, University of Birmingham, Birmingham, UK

[2] Department of Biochemistry, Stellenbosch University, Stellenbosch, South Africa

[3] Molecular Cell Physiology, Vrije Universiteit Amsterdam, Amsterdam, The Netherlands

[4] Upper GI Unit and Minimally Invasive Unit, Heartlands Hospital, University Hospitals Birmingham NHS Foundation Trust, Birmingham, UK

[5]Emerging Innovations Unit, Discovery Sciences, BioPharmaceuticals R&D, AstraZeneca, Cambridge, UK

[6] Leeds Institute of Cardiovascular and Metabolic Medicine, University of Leeds, Leeds, UK

[7] NIHR Leeds Biomedical Research Center, Leeds Teaching Hospitals, NHS Trust, Leeds, UK

[8] Institute of Clinical Sciences, Faculty of Medicine, Imperial College, London, UK

[9] Medical Research Council London Institute of Medical Sciences, London, UK

[#]Shared first authors.

Correspondence:

Karl-Heinz Storbeck, Department of Biochemistry, Stellenbosch University, Private Bag X1, Matieland, 7602, South Africa

Email: storbeck@sun.ac.za

Phone: +27 21 808 5862

Abstract

Aldo-keto reductase 1C3 (AKR1C3) is a key enzyme in the activation of both classic and 11-oxygenated androgens. In adipose tissue, AKR1C3 is co-expressed with 11β-hydroxysteroid dehydrogenase type 1 (HSD11B1), which catalyses the local activation of glucocorticoids but also the inactivation of 11-oxygenated androgens, and thus has the potential to counteract AKR1C3. Using a combination of *in vitro* assays and *in silico* modelling we show that HSD11B1 attenuates the biosynthesis of the potent 11-oxygenated androgen, 11-ketotestosterone, by AKR1C3. Employing *ex vivo* incubations of human female adipose tissue samples we show that inhibition of HSD11B1 results in the increased peripheral biosynthesis of 11-ketotestosterone. Moreover, circulating 11KT increased 2-3 fold in individuals with type 2 diabetes after receiving the selective oral HSD11B1 inhibitor AZD4017 for 35 days, thus confirming that HSD11B1 inhibition results in systemic increases in 11KT concentrations. Our findings show that HSD11B1 protects against excess 11KT production by adipose tissue, a finding of particular significance when considering the evidence for adverse metabolic effects of androgens in women. Therefore, when targeting glucocorticoid activation by HSD11B1 inhibitor treatment in women, the consequently increased generation of 11-ketotestosterone may offset beneficial effects of decreased glucocorticoid activation.

Keywords: Aldo-keto reductase 1C3 (AKR1C3); 11-ketotestosterone; intracrinology; adipose tissue; metabolic syndrome

45 **Graphical Abstract**

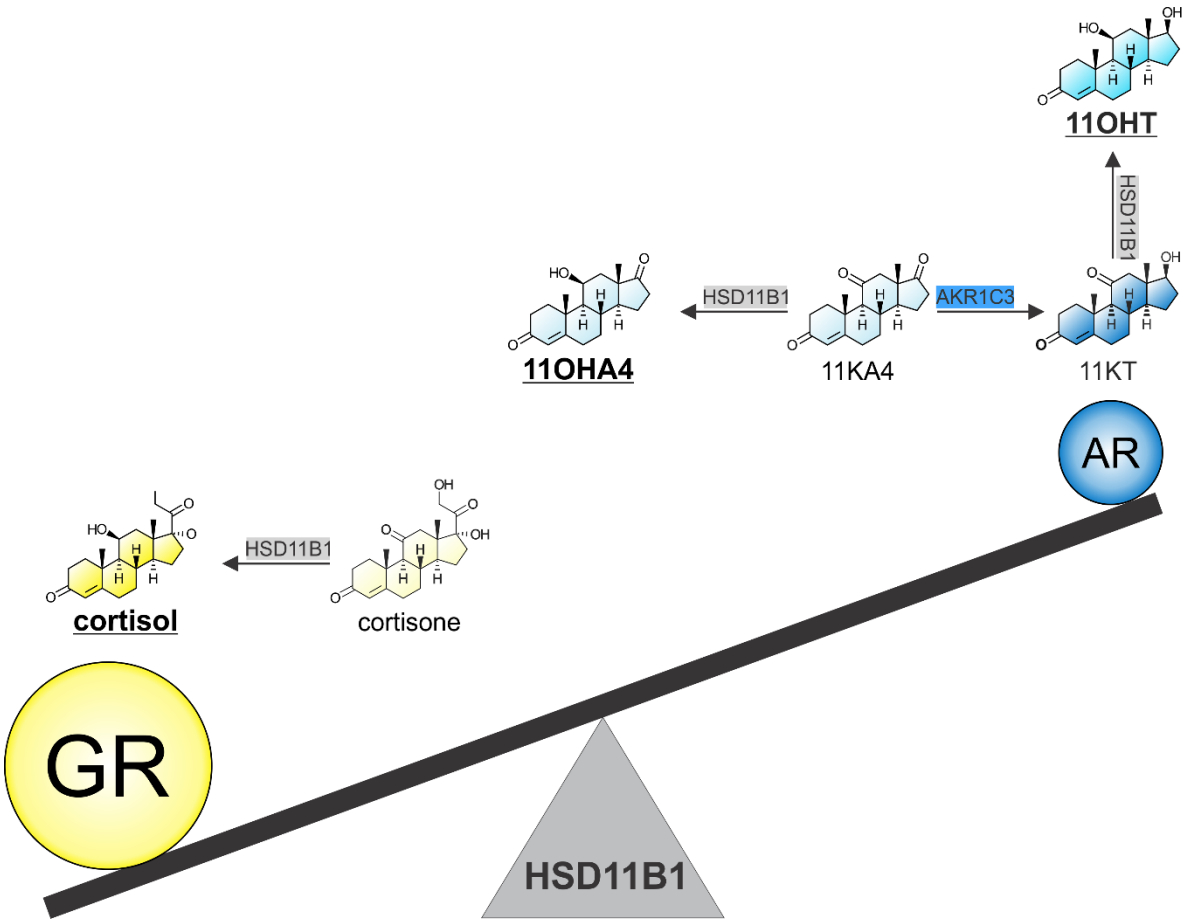

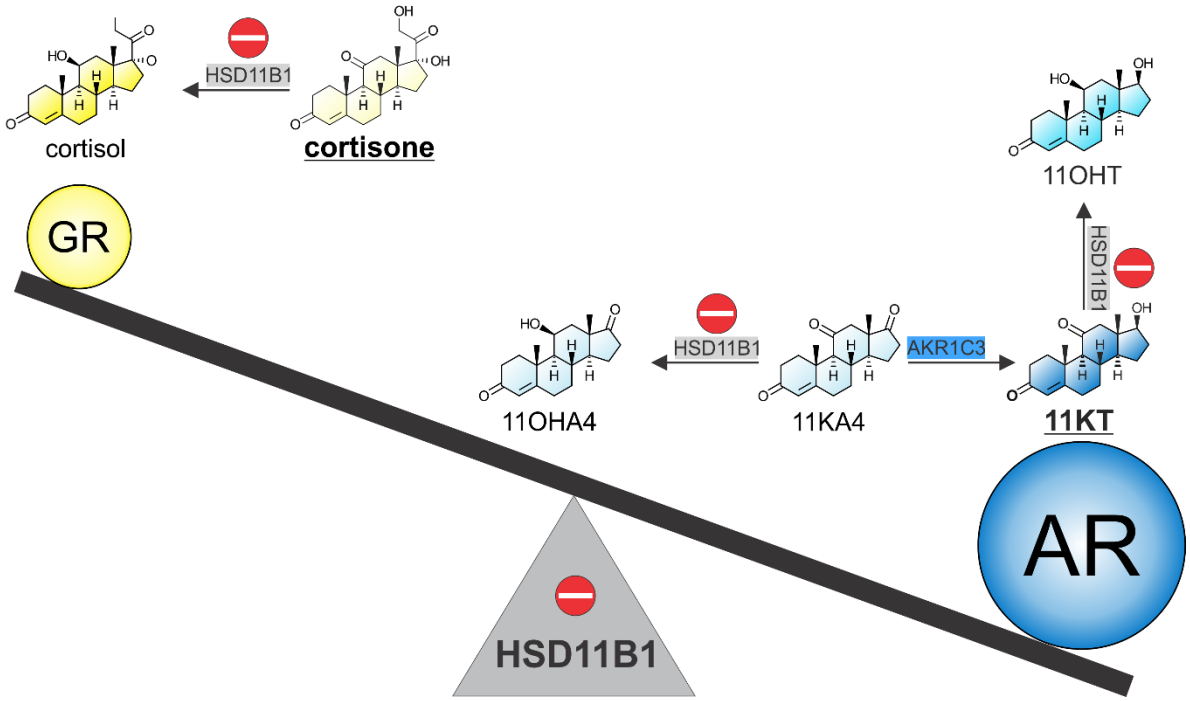

46

47 **Introduction**

48 The 11-oxygenated androgens are a group of adrenal-derived and peripherally activated androgens
49 that make a significant contribution to the circulating androgen pool, particularly in women (>>>). The
50 most potent 11-oxygenated androgen in circulation is 11-ketotestosterone (11KT), which has been
51 shown to bind to and activate the androgen receptor with an affinity and potency similar to
52 testosterone (5). Moreover, several studies have also shown that 11KT circulates at concentrations
53 equal to or higher than those of testosterone in women (3, 6, 7). Unlike the classic androgens, 11-
54 oxygenated androgens do not decline with age, with the result that 11KT is the most abundant active
55 androgen in the circulation of postmenopausal women (3, 6). While the role of 11-oxygenated
56 androgens in healthy individuals has yet to be defined, these androgens have been shown to play a
57 role in disease states such as polycystic ovary syndrome (PCOS), congenital adrenal hyperplasia (CAH),
58 Cushing's syndrome and castration resistant prostate cancer (CRPC) (8–12).

59 The biosynthesis of 11KT begins in the adrenal, where cytochrome P450 11B1 (CYP11B1) catalyses the
60 11β-hydroxylation of locally produced androstenedione to yield 11β-hydroxyandrostenedione
61 (11OHA4). 11OHA4 is released into circulation, and serves as the primary precursor for the
62 biosynthesis of 11KT by peripheral tissues (**Figure 1**). Specifically, 11OHA4 is converted to 11-
63 ketoandrostenedione (11KA4) by mineralocorticoid target tissues expressing 11β-hydroxysteroid
64 dehydrogenase type 2 (HSD11B2), such as the kidney (1>). 11KA4 then subsequently serves as the
65 substrate for the key androgen activating enzyme, aldo-keto reductase 1C3 (AKR1C3), which is
66 abundantly expressed in adipose tissue (14–17). Notably, AKR1C3 catalyses the conversion of 11KA4
67 to 11KT significantly more efficiently than that of androstenedione to testosterone (16, 17). The
68 biosynthesis of 11KT is, however, more complex than that of testosterone as the presence of the 11-
69 keto group makes both 11KA4 and 11KT substrates for 11β-hydroxysteroid dehydrogenase type 1
70 (HSD11B1)—an enzyme best known for amplification of glucocorticoid signalling, which it achieves by
71 converting the inactive cortisone to active cortisol in key metabolic tissues including the liver, adipose
72 tissue and skeletal muscle (11, 18–20). Given that AKR1C3 and HSD11B1 are co-expressed in adipose
73 tissue, we propose that HSD11B1 regulates the amount of 11KT produced in two ways. First, by

74 competing with AKR1C3 for 11KA4, thereby limiting the amount of 11KA4 converted to 11KT by
75 AKR1C3. Secondly, by converting some of the 11KT formed to the far less androgenic 11β-
76 hydroxytestosterone (11OHT) (11) (**Figure 1**). Indeed, while investigating the metabolism of 11KA4 in
77 differentiated Simpson-Golabi-Behmel syndrome preadipocyte (SGBS) cells Paulukinas et. al. noted
78 that HSD11B1 may be protective of androgen excess (17).

79 This proposed mechanism is important when considering that HSD11B1 has long been a therapeutic
80 target for prevention of tissue-specific excess glucocorticoid exposure and treatment of related
81 adverse metabolic effects (19, 21–24). Promising preclinical studies in rodents, which crucially do not
82 produce 11-oxygenated androgens (25–30), were unable to accurately model competing HSD11B1
83 and AKR1C3 effects in humans. Our proposed hypothesis could provide an explanation for the more
84 limited effect sizes observed in clinical trials with HSD11B1 inhibitors (31, 32, 41, 42, 33–40), as
85 increased 11KT production resulting from HSD11B1 inhibition could counteract beneficial effects of
86 reduced glucocorticoid signalling, by increasing androgen signalling. This is particularly significant in
87 women where elevated androgens are linked to insulin resistance, type 2 diabetes, hypertension,
88 cardiovascular disease and metabolic dysfunction associated steatotic liver disease (MASLD), in
89 particular in the context of polycystic ovary syndrome, for which androgen excess is a defining feature
90 (43–52).
91 Here, we characterised the interplay between HSD11B1 and AKR1C3 as co-regulators of 11KT
92 biosynthesis using a combination of *in vitro*, *in silico*, and human *ex vivo* and *in vivo* approaches
93 including selective HSD11B1 inhibitor treatment in individuals with type 2 diabetes.
94

95 **Materials and Methods**

96 **Steroids and inhibitors**

97 Androstenedione (4-androstene-3,17-dione), carbenoxolone ((3β,20β)-3-(3-carboxy-1-oxopropoxy)-
98 11-oxo-olean-12-en-29-oic acid, disodium salt; CBX), cortisol (11β,17α,21-trihydroxypregn-4-ene-3,20-
99 dione), cortisone (17α,21-dihydroxy-4-pregnene-3,11,20-trione), DHEA (5-androsten-3β-ol-17-one),
100 DHEA sulfate (5-androsten-3β-ol-17-one-3-sulfate) and testosterone (4-androsten-17β-ol-3-one) were

101 purchased from Sigma Aldrich. 11β-hydroxyandrostenedione (11β-hydroxy-4-androstene-3,17-dione),
102 11β-hydroxytestosterone (11β,17β-dihydroxyandrost-4-en-3-one), 11-ketoandrostenedione (4-
103 androsten-3,11,17-trione) and 11-ketotestosterone (4-androsten-17β-ol-3,11-dione) were from
104 Steraloids. The deuterated internal standards 11β-hydroxyandrostenedione-2,2,4,6,6,16,16-D7 (D7-
105 11OHA4), 11-ketotestosterone-16,16,17-D3 (D3-11KT), androstenedione-2,2,4,6,6,16,16-D7 (D7-A4),
106 cortisol-9,11,12,12-D4 (D4-F), DHEAS-16,16-D2 (D2-DHEAS) and testosterone-16,16,17-D3 (D3-T) were
107 all purchased from Cambridge Isotope Laboratories. Dehydroepiandrosterone-2,2,3,4,4,6-D6 (D6-
108 DHEA) and cortisone-2,2,4,6,6,9,12,12-D8 (D8-E) were purchased from Sigma Aldrich, while 11-
109 ketoandostenedione-2,2,4,6,6,9,12,12,16,16-D10 (D10-11KA4) was custom synthesized by Toronto
110 Research Chemicals. The selective HSD11B1 inhibitor, 2-[(3S)-1-[5-(cyclohexylcarbamoyl)-6-
111 propylsulfanylpyridin-2-yl]-3-piperidyl] acetic acid (AZD-4017) was provided by AstraZeneca.

112 **Plasmids**

113 The pcDNA3 vector containing AKR1C3 was provided by Prof. J. Adamski (Helmholtz Zentrum
114 München, Germany). The pcDNA3 vectors containing HSD11B1 and hexose 6-phosphate
115 dehydrogenase (H6PDH) were from Prof. K. Chapman (University of Edinburgh, UK). The pTAT-GRE-
116 Elb-luc luciferase promoter reporter construct, containing two copies of the GRE was from Prof. G.
117 Jenster (Erasmus University of Rotterdam, Netherlands), while the GR expressing plasmid (pRShGRα)
118 was from Prof. R. Evans (Howard Hughes Medical Institute, La Jolla, USA). The pCIneo plasmid
119 expressing the wild-type human AR was from Prof. N. Sharifi (Cleveland Clinic, Cleveland, USA). A
120 pCIneo plasmid, containing no cDNA insert, was purchased from Promega (Wisconsin, USA).

121 **Cell lines**

122 HEK293 cells were purchased from the American Type Culture Collections (ATCC) and cultured in high
123 glucose Dulbecco's Modified Eagle Medium (DMEM) supplemented with 10% FBS, 1.5 g/L $NaHCO_3$ and
124 1% penicillin-streptomycin and maintained at 37 °C in 90% humidity and 5% CO^2. The cells were
125 authenticated by short-tandem repeat profiling (NorthGene) and were regularly tested for
126 mycoplasma contamination.

127 **Determining kinetic parameters for HSD11B1 and computational model construction**

128 The kinetic parameters ($K_{m,\ app}$ and $V_{max,\ app}$) for HSD11B1 were determined using the methodology
129 previously reported for AKR1C3 (1>). Briefly, HEK293 cells were seeded into 10 cm^2 tissue culture
130 dishes at a density of $2x10^5$ cells per mL (10 mL per dish). After a 24 hour incubation period, cells were
131 co-transfected with 0.5 µg HSD11B1 and 0.5 µg H6PDH DNA using X-tremeGENE™ HP DNA transfection
132 reagent (Roche) according to manufacturer's protocol. Following a 24 hour incubation the transfected
133 cells were re-plated into 48-well Corning® CELLBIND® plates at a density of $2x10^5$ cells per mL (300 µL

134 per well). Cells were incubated for an additional 24 hours to allow for attachment before being treated
135 with serum free media, containing appropriate steroid substrate (cortisone, 11KA4, or 11KT) at
136 concentrations ranging from 0.1 µM to 10 µM. Aliquots (250 µL) for the quantification of steroid
137 metabolism by ultra-high performance liquid chromatography tandem mass spectrometry (UHPLC-
138 MS/MS) were collected at specific time intervals. Kinetic parameters were determined in Wolfram
139 Mathematica (Version 13) by assuming Michaelis Menten kinetics and fitting the $K_{m,\ app}$ and $V_{max,\ app}$
140 values by minimizing the sum of the squared differences between the experimentally determined
141 progress curves and model, weighted by the variance using the NMinimize function. The model was
142 fitted to triplicate data from three independent experiments. The transfection efficiency of each
143 individual experiment was taken into account by determining the initial rate of the conversion of 100
144 nM 11KA4 for each independent experiment. A computational model containing the determined
145 kinetic for HSD11B1 and those previously determined for AKR1C3 was subsequently constructed. This
146 model is comprised of ordinary differential equations (ODEs) for the metabolites, and numerical
147 integration by making use of the NDSolve routine in Mathematica allowed for experimentally
148 comparable metabolite profiles to be obtained. Additionally, the model was used to predict the
149 conversion of cortisone or 11KA4 for varying HSD11B1:AKR1C3 ratios, see Supplementary material for
150 a complete model description and simulation details.

151 **Determining the effect of different HSD11B1:AKR1C3 ratios on cortisone and 11KA4 metabolism**

152 HEK293 cells were seeded into 10 cm^2 tissue culture dishes at a density of $2x10^5$ cells per mL (10 mL
153 per dish). After a 24 hour incubation period, dishes were co-transfected with either 0.5 µg HSD11B1
154 and 0.5 µg H6PDH or 0.5 µg AKR1C3 and 0.5 µg pCINeo using X-tremeGENE™ HP DNA transfection
155 reagent (Roche). Additional dishes were transfected with 1 µg of the pCINeo (no insert) as to allow for
156 the subsequent plating of an equal number of transfected cells at all HSD11B1:AKR1C3 ratios. After 24
157 hours cells were counted and combined in different ratios of HSD11B1:AKR1C3, before being re-plated
158 into 12-well Corning® CELLBIND® surface plates at a density of $4x10^5$ cells per mL (1 mL per well). After
159 an additional incubation period of 24 hours, the media was replaced with serum free DMEM containing
160 100 nM substrate (11KA4 or cortisone). Aliquots (500 µL) were collected 24 hours after the addition of
161 substrate for analysis by UHPLC-MS/MS, as described below.

162 **Determining the effect of CBX on HSD11B1 and AKR1C3 co-expression**

163 HSD11B1 and AKR1C3 transfections were performed as described above. Transfected cells were
164 re-plated at a 1:1 ratio of HSD11B1:AKR1C3 ($2x10^5$ cells/mL, 300 µL) in 48-well Corning® CELLBIND®
165 surface plates. After 24 hours, media was replaced with serum free media containing 100 nM cortisone
166 in combination with either 10 nM or 100 nM 11KA4 in the absence and presence of 10 µM CBX.
167 Aliquots (200 µL) were collected over a 24 hour period for analysis by UHPLC-MS/MS.

168 **Promoter reporter assays**

169 To determine the effect of the HSD11B1 inhibitor CBX on AR and GR transactivation, HSD11B1 and
170 AKR1C3 transfections were performed 24 hours before co-transfections of HEK293 cells with either a
171 AR expression plasmid (0.09 µg) and the pTAT-GRE-Elb-luc luciferase promoter reporter construct (0.9
172 µg) or a GR expression plasmid (0.09 µg) and the pTAT-GRE-Elb-luc luciferase promoter reporter
173 construct (0.9 µg). HSD11B1 and AKR1C3 transfected cells were re-plated at a 1:1 ratio ($4x10^5$ cells/mL,
174 1 mL) in 12-well Corning® CELLBIND® surface plates. Following 24 hours, media was replaced with
175 serum free media containing 100 nM cortisone and 10 nM 11KA4 in the absence and presence of 10
176 µM CBX. At the same time the AR-GRE transfected cells and GR-GRE transfected cells were re-plated
177 into 48-well Corning® CELLBIND® plates ($3x10^5$ cells/mL, 300 µL). Following a 24 hour incubation with
178 steroid, aliquots (200 µL) from the HSD11B1:AKR1C3 expressing cells were collected for analysis of
179 steroid metabolism by UHPLC-MS/MS. A further 300 µL conditioned media was transferred to each of
180 the AR-GRE and GR-GRE transfected cells. These cells were incubated for a further 24 hours after which
181 cell lysates were harvested in passive lysis buffer. Reporter activity was then measured by making use
182 of the Luciferase Assay System (Promega). The luciferase values were normalised to the protein
183 concentration of each individual sample determined using a Thermo Scientific™ Pierce™ BCA Protein
184 Assay kit.

185 **Determining the effect of ADZ4017 on 11KA4 conversion in human adipose tissue**

186 Paired subcutaneous and omental adipose tissue was collected from eight female participants (age
187 range 32-59 years, BMI range 42-57 kg/m^2) undergoing elective abdominal non-cancer surgery (Black
188 Country Research Ethics Committee references 14/WM/0011 and 19/WM/0183). Written, informed
189 consent was obtained prior to surgery and sample collection. Adipose tissue samples were transported
190 to the laboratory at room temperature in DMEM/F12 supplemented with 33 µM biotin, 17 µM
191 panthotenic acid and 1% penicillin-streptomycin. Connective tissue and vessels were removed and the
192 adipose tissue washed in PBS. Tissue samples of 100-300 mg were cut and weighed. Each sample was
193 cut into four smaller pieces for incubations with 100 nM cortisone or 100 nM 11KA4 in the presence
194 and absence of 100 nM HSD11B1 inhibitor AZD4017 in DMEM/F12-Ham (supplemented as described
195 above). Final solvent concentrations were adjusted to 0.00302% MeOH and 0.1% DMSO in all
196 incubations. Tissue incubations were constantly rotated in a hybrid oven at 37 °C for 72 hours. Medium
197 samples were centrifuged for 10 minutes at 16,000g and 4 °C and the supernatant was used for analysis
198 of steroid metabolism by UHPLC-MS/MS. The tissue was washed in PBS, snap frozen in liquid nitrogen
199 and stored at -80 °C for RNA extraction.

200

201 **RNA isolation and gene expression analysis from HEK293 cells**

202 Total RNA was isolated from cells using Tri-Reagent® (Sigma) and cDNA synthesis carried out using the
203 GoScript™ Reverse Transcription System kit (Promega). Quantitative PCR was performed using a Roche
204 LightCycler® 96 rapid thermal cycler instrument and the KAPA SYBR® FAST qPCR Master Mix for
205 LightCycler®. Primer sequences as follows, AKR1C3 (forward) 5'- AGCCAGGTGAGGAACTTTC-3' (53),
206 AKR1C3 (reverse) 5'- ATCACTGTTAAAATAGTGGAG-3' (53), HSD11B1 (forward) 5'-
207 CTGCCTGCTTAGGAGGTTGT-3', HSD11B1 (reverse) 5'- CCTTGGAGCATCTCTGGTCTG-3', the reference
208 gene ubiquitin conjugating enzyme (UBC) (forward) 5'- CCGGGATTTGGGTCGCAG-3', UBC (reverse) 5'-
209 TCACGAAGATCTGCATTGTCAAG-3'. Primer efficiencies were between 90% and 110% for all primer sets.
210 Relative gene expression was calculated using a modified form of the model described by Pfaffl (54).
211 Inter-experimental variations were adjusted using a mean-centering (55).

212 **RNA isolation and gene expression analysis from adipose tissue**

213 Adipose tissue was homogenised in Tri-Reagent® and total RNA was isolated after phenol-chloroform
214 extraction using the Qiagen RNeasy Mini Kit using an established protocol (56). Reverse transcription
215 was performed using Applied Biosystems™ TaqMan™ Reverse Transcription Reagents according to the
216 manufacturer's protocol. qPCR was performed on an ABI 7900HT sequence detection system (Perkin
217 Elmer, Applied Biosystems) using TaqMan™ Gene Expression Assays (FAM-labelled) and the
218 SensiFAST™ Probe Hi-ROX kit (Bioline). The following TaqMan™ Gene Expression Assays were used:
219 18S Hs99999901_s1, AKR1C3 Hs00366267_m1, HSD11B1 Hs01547870_m1.

220 **Determining the effect of ADZ4017 glucocorticoid and androgen concentrations *in vivo***

221 A total of 28 participants (22 male and 6 female), all with type 2 diabetes, were recruited for a
222 randomized, double-blind, parallel-group, placebo-controlled trial. Full ethical approval was acquired
223 from North West Greater Manchester Central Research Ethics Committee 17/NW/0283 prior to the
224 initiation of recruitment for the study. Informed consent was obtained from all participants after the
225 nature and possible consequences of the study had been explained. Participants received either oral
226 AZD4017 (400 mg) or a matched oral placebo twice daily for 35 days. Blood samples and urine were
227 collected from individuals before first treatment and after completion of the trial and were analysed
228 by UHPLC-MS/MS and GC-MS, respectively. Refer to Ajjan *et al.* (40) for further details on study design
229 and participants.

230 **Steroid extraction**

231 Steroids were extracted from HEK293 tissue culture media using Tert-butyl methyl ether (MTBE) (57).
232 In brief, following the addition of an internal standard mix (100 µL containing 2 ng D3-T and 5 ng D7-

233 A4, D7-11OHA4, D3-11KT and D4-F in acetonitrile) and MTBE (3:1 ratio of MTBE:media), samples were
234 vortexed at 1 500 rpm for 10 minutes, after which they were incubated at -80 °C for 1 hour, allowing
235 for the aqueous layer to freeze. The resulting organic phase was subsequently transferred to a clean
236 test tube and evaporated under a stream of nitrogen gas at 45 °C. Extracted steroids were then
237 reconstituted by the addition of 50% (v/v) methanol and stored at -20 °C until analysis by UHPLC-
238 MS/MS. Serum steroids and steroids in medium adipose tissue incubations were extracted using a
239 similar method. Samples (200 µL for serum, 500 µL for adipose tissue conditioned medium) were mixed
240 with 10 µL internal standards in 50% (v/v) methanol in water (D4-F, D8-E, D6-DHEA, D7-A4, D3-T, D7-
241 11OHA4, D10-11KA4, D3-11KT; 5 ng each for serum, 20 ng each for adipose tissue). For serum samples
242 50 µL acetonitrile were added for protein precipitation prior to extraction and the samples vortexed.
243 MTBE was added to each sample (1 mL for serum; 3 mL for medium from adipose tissue incubations)
244 and the samples were vortexed at 1000 rpm for 10 min. Following incubation at room temperature for
245 30 minutes the organic phase was transferred, dried under a stream of nitrogen gas at 45 °C and
246 reconstituted with 50% (v/v) methanol in water prior to analysis by UHPLC-MS/MS. For the
247 measurement of serum DHEAS, 200 ng D2-DHEAS in 20 uL of 50% methanol was added to 20 µL of
248 serum followed by 20 µL of 1 mM $ZnSO_4$ and 100 µL acetonitrile. The samples were centrifuged and
249 100 µL of the supernatant was dried and reconstituted in 50% (v/v) methanol in water prior to UHPLC-
250 MS/MS analysis.

251 **Quantification of steroids by ultra-high performance liquid chromatography tandem mass**
252 **spectrometry (UHPLC-MS/MS)**

253 Steroids from assays performed in HEK293 cells were separated and quantified using a UPLC high
254 strength silica (HSS) T3 column (2.1 mm X 50 mm, 1.8 µm particle size) coupled to an ACQUITY UPLC
255 and Xevo TQ-S triple quadrupole mass spectrometer (Waters Corporation, Milford, USA) as previously
256 reported (57). Steroids extracted from serum or adipose tissue incubations were separated and
257 quantified using Phenomenex Luna Omega polar C18 column (2.1 X 50 mm, 1.6 µm particle size;
258 Phenomenex, Macclesfield, UK) coupled to an ACQUITY UPLC and a Waters Xevo TQ-XS triple
259 quadrupole mass spectrometer as previously described (58). Serum DHEAS was quantified using a HSS
260 T3 column (2.1 X 50 mm, 1.8 µm particle size; Waters) coupled to an ACQUITY UPLC and a Waters Xevo
261 TQ-XS triple quadrupole mass spectrometer as previously described (59, 60).

262 **Quantification of urinary steroids by GC-MS**

263 Measurement of urinary steroid metabolite excretion was carried out by a long-established gas
264 chromatography-mass spectrometry (GC-MS) method (61). In brief, free and conjugated steroids were
265 extracted from 1 mL urine by solid-phase extraction. Steroid conjugates were enzymatically

266 hydrolyzed, reextracted, and chemically derivatized to form methyloxime trimethyl silyl ethers. An
267 Agilent 5975 instrument operating in selected-ion-monitoring (SIM) mode achieved sensitive and
268 specific detection and quantification of selected steroid metabolites.

269 **Statistical analysis**

270 We performed unpaired t-tests to compare the effect of HSD11B1 inhibition on 11-oxygenated
271 androgen production in HEK293 cells expressing AKR1C3 and HSD11B1 and on the transactivation of
272 the androgen receptor. Paired t-tests were performed to assess the effect of HSD11B1 inhibition in
273 adipose tissue, while Wilcoxon signed-rank tests were used to assess the effect in serum and urine.
274 Correlations between serum steroid concentrations and clinical outcomes were investigated using a
275 Spearman's Rho test.

276

277 **Results**

278 **HSD11B1 efficiently catalyses the 11β-reduction of 11-oxygenated androgens.**

279 Non-steroidogenic HEK293 cells were transiently transfected to express HSD11B1 and activity assayed.
280 Rate equations were fitted to the progress curves for three independent experiments as shown in
281 **Supplementary Figure 1**. A low but detectable reverse reaction rate was observed for the cortisone to
282 cortisol and the 11KA4 to 11OHA4 reactions. Reversible kinetics were therefore used for these
283 reactions. Our results show that the apparent K_m ($K_{m,\ app}$) of HSD11B1 for cortisone and 11KA4 are
284 similar (0.9 µM and 1 µM), while the $K_{m,\ app}$ for 11KT (0.21 µM) is >4-fold lower, indicating a higher
285 affinity towards 11KT (**Table 1**). However, the apparent V_{max} ($V_{max,\ app}$) for 11KT (0.05 µM/h) was >2-
286 fold lower than that for cortisone (0.12 µM/h) and 7-fold lower than that for 11KA4 (0.35 µM/h).
287 Considering the V_{max}/K_m values, an estimate of enzyme efficiency, both 11KA4 and 11KT are more
288 efficiently converted to their respective products than the traditionally recognised HSD11B1 substrate
289 cortisone.

290

291 **Co-expression of HSD11B1 with AKR1C3 modulates the activation of 11-oxygenated androgens.**

292 AKR1C3 is the key enzyme catalysing the peripheral conversion of androgen precursors into active
293 androgens (1>). We have previously shown that AKR1C3 catalyses the conversion of 11KA4 to the

294 potent androgen 11KT 8-fold more efficiently than the conversion of androstenedione to testosterone
295 (16). To determine how the co-expression of HSD11B1 with AKR1C3 would affect 11KT production, we
296 mixed transfected HEK293 cells expressing either AKR1C3 or HSD11B1 to obtain increasing ratios of
297 HSD11B1:AKR1C3, while keeping the number of cells expressing AKR1C3 constant. The total cell count
298 was also kept constant by including cells transfected with an empty plasmid as required. The relative
299 expression of HSD11B1:AKR1C3 was confirmed by qPCR (**Figure 2A**). Increased ratios of
300 HSD11B1:AKR1C3 resulted in increased concentrations of cortisol being produced upon addition of
301 100 nM cortisone (**Figure 2B**), thereby confirming the increased HSD11B1 expression. Similarly,
302 increasing the ratio of HSD11B1:AKR1C3 resulted in the concomitantly increased production of
303 11OHA4 from 11KA4, with 11OHA4 becoming the most abundant product when the HSD11B1:AKR1C3
304 ratio was increased beyond 0.1:1 (**Figure 2C**). Biosynthesis of 11KT was highest when AKR1C3 was
305 expressed in the absence of HSD11B1, with increasing HSD11B1:AKR1C3 ratios resulting in a rapid
306 decrease in the concentrations of 11KT. 11OHT initially increased as the ratio of HSD11B1:AKR1C3
307 increased, peaking at a ratio of 0.25:1. Further increases in the HSD11B1:AKR1C3 ratio resulted in
308 decreased concentrations of 11OHT being produced.
309 Using the parameterised rate equations for HSD11B1 and those previously determined by us for
310 AKR1C3 (1>), a computational model consisting of a set of ordinary differential equations was
311 constructed to simulate steroid metabolism in cells with both enzymes expressed:
312 $$\frac{d\,\mathrm{ka4}(t)}{d\,\mathrm{t}} = -v_{\mathrm{HSD_ka4}} - v_{\mathrm{AKR_ka4}};\ \frac{d\,\mathrm{oha4}(t)}{d\,\mathrm{t}} = v_{\mathrm{HSD_ka4}};\ \frac{d\,\mathrm{kt}(t)}{d\,\mathrm{t}} = v_{\mathrm{AKR_ka4}} - v_{\mathrm{HSD_kt}};\ \frac{d\,\mathrm{oht}(t)}{d\,\mathrm{t}} = v_{\mathrm{HSD_kt}}$$
313 The rate equations for HSD11B1 and AKR1C3 are given in the Supplementary material. The model was
314 able to predict the experimentally determined effect of increasing HSD11B1:AKR1C3 ratios on the
315 metabolism of cortisone and 11KA4, respectively (**Figure 2**). Note that the kinetic parameters in the
316 mathematical model were not fitted to the experimental data for the different HSD11B1:AKR1C3
317 ratios, but were determined in the progress curves for the individual incubations (**Supplementary**
318 **Figure 1)**. Taken together these data clearly show that HSD11B1 modulates the biosynthesis of 11KT
319 by AKR1C3, and that the model can predict the effect of varying HSD11B1:AKR1C3 ratios.
320

321 ***In vitro* inhibition of HSD11B1 results in the accumulation of 11-ketotestosterone.**

322 Next, we set out to determine the effect of HSD11B1 inhibition on 11KT biosynthesis. We mixed
323 HEK293 cells transiently transfected with either AKR1C3 or HSD11B1 at a ratio of 1:1 and
324 simultaneously treated the cells with cortisone and 11KA4 in the absence and presence of the HSD11B1
325 inhibitor, carbenoxolone (CBX). We used either equimolar concentrations of cortisone and 11KA4 (100
326 nM each) or 10-fold excess of cortisone (100 nM) over 11KA4 (10 nM) to more closely mimic circulating
327 concentrations (>). Our results show that CBX reduced the production of cortisol from cortisone from
328 56.5 nM to 3.2 nM after 24 hours, demonstrating effective HSD11B1 inhibition (**Figure 3A & B**). In the
329 absence of CBX the majority of 11KA4 (69%) was converted to 11OHA4 by HSD11B1, with only 3.8 nM
330 of 11KT produced from 100 nM 11KA4 by AKR1C3 (**Figure 3C**). However, inhibition of HSD11B1 resulted
331 in a 7-fold increase in 11KT production after 24 hours (**Figure 3D**). Similarly, in cells treated with 100
332 nM cortisone and 10 nM 11KA4, inhibition of HSD11B1 by CBX resulted in a 12-fold increase in 11KT
333 production (0.15 nM without CBX to 1.8 nM with CBX) (**Figure 3E & F**). 11KT was the by far most
334 abundant 11-oxygenated androgen following inhibition of HSD11B1. Inhibition of both the conversions
335 from 11KA4 to 11OHA4 and 11KT to 11OHT, respectively, allowed AKR1C3 to catalyse the conversion
336 of 11KA4 to 11KT without the need to compete for substrate and prevented the inactivation of 11KT
337 to the less potent 11OHT. The computational model was able to independently predict the outcome
338 of HSD11B1 inhibition under the experimental conditions (**Figure 3**).

339

340 ***In silico* analysis of the combined effect of HSD11B1:AKR1C3 co-expression and HSD11B1 inhibition**
341 **on 11KT biosynthesis.**

342 After having shown that the computational model was able to individually predict both the effect of
343 increasing HSD11B1:AKR1C3 ratios (**Figure 2**) and the effect of HSD11B1 inhibition (**Figure 3**), we used
344 the model to simultaneously predict the effect of differing HSD11B1 and AKR1C3 expression and
345 differing degrees of HSD11B1 inhibition on the conversion of 10 nM 11KA4 to 11OHA4, 11KT and
346 11OHT after 24 hours (**Figure 4**). These results confirmed that HSD11B1 strongly modulates the
347 biosynthesis of 11KT by competing for the precursor, 11KA4, and by converting the 11KT that is formed

348 to the less potent androgen 11OHT. The inhibition of HSD11B1 reduced these effects under all
349 HSD11B1:AKR1C3 ratios tested leading to increased production of 11KT. Notably, lower ratios of
350 HSD11B1:AKR1C3 were more sensitive to HSD11B1 inhibition, more quickly leading to increased 11KT
351 concentrations as the level of inhibition was increased. Higher absolute concentrations of 11KT were
352 also produced by lower ratios of HSD11B1:AKR1C3 (AKR1C3 was kept constant) when HSD11B1 was
353 inhibited up to the maximum simulated I/Ki value of ten. Near complete inhibition of HSD11B1 (I/Ki =
354 100), however, negated the effect of the HSD11B1:AKR1C3 ratio with 11KT production dependent only
355 on AKR1C3 (**Supplementary Figure 2**). The effect of HSD11B1 inhibition is therefore dependent on the
356 degree of inhibition, the ratio of HSD11B1:AKR1C3 and the absolute expression level of HSD11B1 and
357 AKR1C3.
358 To investigate the potential biological impact of HSD11B1 inhibition, we combined HEK293 cells
359 expressing AKR1C3 or HSD11B1 at a 1:1 ratio and incubated the cells with 100 nM cortisone and 10
360 nM 11KA4 in the absence and presence of CBX for 24 hours. The conditioned media were then
361 transferred to HEK293 cells transiently transfected with either a plasmid expressing the glucocorticoid
362 receptor (GR) or the androgen receptor (AR), and a luciferase reporter construct. The GR- and AR-
363 mediated induction of luciferase was subsequently measured after an additional 24 hour incubation.
364 As expected, HSD11B1 mediated the conversion of cortisone to cortisol, with the resulting cortisol
365 increasing the transactivation of the GR (94-fold induction). Inhibition of HSD11B1 with CBX reduced
366 cortisol production 32-fold (**Figure 5A**) and resulted in a 34-fold decrease in GR transactivation (**Figure**
367 **5B**). Conversely, inhibition of HSD11B1 resulted in a 7-fold increase in transactivation of the AR due to
368 significantly increased 11KT biosynthesis (**Figure 5C & D**). Basal levels of AR transactivation in the
369 absence of CBX and 11KT were due to the presence of low concentrations of 11OHT (0.81 nM;
370 **Supplementary Figure 3**), which is a partial agonist of the AR (11, 62). It should be noted that we
371 observed that CBX weakly antagonises the AR (**Supplementary Figure 4**), hence, the induction of the
372 AR was likely underestimated. Nonetheless, taken together, these data demonstrate that while
373 inhibition of HSD11B1 results in the desired decrease in GR transactivation, this is accompanied by a
374 shift towards AR transactivation.

375

376 **Selective HSD11B1 inhibition increases 11KT production in female human adipose tissue *ex vivo*.**

377 We next set out to determine the effect of HSD11B1 inhibition on 11KT biosynthesis in paired
378 subcutaneous and omental adipose tissue samples from women undergoing elective bariatric surgery.
379 For these experiments we employed the selective HSD11B1 inhibitor AZD4017 (63). The conversion of
380 cortisone to cortisol was reduced to 3% of the uninhibited conversion rate in subcutaneous adipose
381 tissue treated with AZD4017, thereby confirming effective HSD11B1 inhibition (**Figure 6A**). Following
382 incubation of subcutaneous adipose tissue with 11KA4 (100 nM), the most abundant product formed
383 in the absence of AZD4017 was 11OHT (60.1% of total products formed), followed by 11OHA4 (23.4%)
384 and 11KT (16.5%) (**Figure 6F**). The biosynthesis of both 11KT and 11OHT is dependent on AKR1C3
385 activity and the observed sum of 11KT and 11OHT (76.6% of products formed) suggested substantial
386 AKR1C3 expression. This was confirmed by qPCR analysis, which showed higher AKR1C3 expression
387 relative to that of HSD11B1 (**Figure 6C**). However, HSD11B1 converted 78.5% of the 11KT formed to
388 the less active 11OHT. Inhibition of HSD11B1 by AZD4017, resulted in a 5-fold increase in 11KT, with
389 11KT becoming the most abundant product (85.6%) (**Figure 6G**). This was accompanied by significant
390 decreases in the production of both 11OHA4 and 11OHT (21-fold and 4.5-fold, respectively).
391 Marginally lower conversion of cortisone to cortisol was observed in omental adipose tissue as
392 compared to subcutaneous tissue, with AZD4017 again effectively inhibiting HSD11B1 activity (**Figure**
393 **6B**). Treatment with AZD4017 again resulted in a significant decrease in 11OHA4 and 11OHT
394 concentrations, with an accompanying 4-fold increase in 11KT production (**Figure 6H & I**).
395 The sum of 11KT and 11OHT (66.0%) was lower in the omental tissue than in subcutaneous tissue
396 (76.6%) illustrating lower AKR1C3 expression as confirmed by qPCR (**Figure 6C & D**). The ratio of
397 HSD11B1 over AKR1C3 expression was lower in subcutaneous than omental adipose tissue (**Figure 6E**),
398 favouring androgen activation in subcutaneous tissue vs glucocorticoid activation in omental tissue.
399 The metabolism of 11KA4 and the effect of AZD4017 inhibition in human adipose tissue was simulated
400 with the mathematical model that was constructed using conversion data obtained from transfected
401 HEK293 cells. The expression levels of the HSD11B1 and AKR1C3 in the adipose tissue relative to that

402 in transfected HEK293 cells therefore needed to be estimated. This was achieved by fitting the
403 expression levels of HSD11B1 to the cortisone to cortisol conversion data (**Figure 6A & B**) and then
404 using an AKR1C3 activity based on the AKR1C3/HSD11B1 expression ratio as determined by qPCR
405 (**Figure 6C & D**). This allowed the model to predict the conversion of 11KA4 to the respective products
406 over time. These simulation revealed the initial accumulation of 11KT, prior to the time dependent
407 conversion of this product to 11OHT by HSD11B1 (**Figure 6F &H**). Inhibition of HSD11B1 eliminated the
408 latter conversion yielding only 11KT and illustrated that the amount of 11KT formed over time was
409 dependent on the absolute expression levels of AKR1C3.
410 Taken together, these data indicate that inhibition of HSD11B1 in adipose tissue leads to a shift in the
411 metabolism of 11-oxygenated androgens resulting in increased 11KT biosynthesis.
412
413 ***In vivo* treatment with a selective HSD11B1 inhibitor increases circulating 11KT concentrations.**
414 After having shown that inhibition of HSD11B1 in adipose tissue shifts the metabolism of 11-
415 oxygenated androgens towards 11KT biosynthesis, we next set out to determine if inhibition of
416 HSD11B1 would alter circulating concentrations of 11KT. We therefore measured a panel of 11-
417 oxygenated androgens as well as cortisol and cortisone in the serum of individuals with type 2 diabetes
418 who had received treatment with the selective HSD11B1 inhibitor AZD4017 during a randomized,
419 double-blind, parallel-group, placebo-controlled phase 2b pilot trial (40). Paired (day 0 and day 35)
420 samples were available for 18 participants (13 men and 5 women; median BMI 32.2 kg/m^2 range 25.0-
421 47.5 kg/m^2; median age 64.5, range 28-84 years), with 11 randomised to HSD11B1 inhibitor treatment
422 (7 men and 4 women) and 7 (6 men and 1 woman) to placebo.
423 Our measurements confirmed that AZD4017 significantly reduced the serum cortisol/cortisone ratio,
424 indicating effective HSD11B1 inhibition as previously reported for selected urinary glucocorticoid
425 metabolites by LC-MS/MS (40), and further confirmed here by GC-MS **(Supplementary Figure 5)**.
426 However, concomitantly, circulating 11KT concentrations significantly increased 2.5-fold (from 1.7 to
427 4.3 nM) following treatment with 400 mg AZD4017 twice daily for 35 days. This was accompanied by
428 a significant, 2-fold decrease in 11OHT concentrations and a 4-fold decrease in the 11OHT/11KT ratio

429 **(Figure 7)**. While the circulating concentrations of the 11-oxygenated androgen precursors 11OHA4
430 and 11KA4 did not change, a small, but significant decrease was also observed for the 11OHA4/11KA4
431 ratio. These changes were also reflected by a significant increase in the urinary metabolite 11-
432 oxoandrosterone, which is derived from 11KA4 and 11KT (64), and a 6-fold decrease in the 11β-
433 hydroxyandrosterone/11-oxoandrosterone ratio **(Figure 7)**. No changes in the serum concentrations
434 of 11-oxygenated androgens were observed in the placebo-treated group (**Supplementary Figure 6**).
435
436 When considering correlations between the changes in circulating steroid concentrations, it is
437 interesting to note that the cortisol/cortisone ratio is highly correlated with the change in both the
438 ratios of 11OHA4/11KA4 ($R = 0.893$; $P < 0.001$) and 11OHT/11KT ($R = 0.686$; $P < 0.01$), but not with the
439 change in circulating 11KT ($R = -0.375$; $P = 0.126$) (**Supplementary Table 1**).
440

441 **Discussion**

442 The relatively recent identification of 11-oxygenated androgens as important contributors to the
443 human androgen pool has prompted a re-evaluation of existing paradigms. One such paradigm is the
444 idea that the two HSD11B isoforms are predominantly involved in the peripheral metabolism of
445 glucocorticoids. We and others have previously shown that HSD11B1 and HSD11B2 are essential for
446 the interconversion of the 11β-hydroxyl and 11-keto forms of the 11-oxygenated androgens (11, 20).
447 We have also previously shown that 11KA4, but not 11OHA4, is a substrate for the key androgen-
448 activating enzyme AKR1C3 (16, 17). Therefore, HSD11B2 plays a vital role in catalysing the conversion
449 of adrenal-derived 11OHA4 to 11KA4, which can then be converted to the potent androgen 11KT by
450 AKR1C3 (13). One of the main sites of AKR1C3 expression and peripheral androgen activation is
451 adipose tissue (14, 15) which also abundantly expresses HSD11B1 (19, 22, 65). Paulukinas et. al. have
452 previously observed that co-expression of HSD11B1 with AKR1C3 in differentiated SGBS adipocyte cells
453 may prevent the accumulation of 11KT, thus suggesting that HSD11B1 may protect from androgen
454 excess (17). Here, using a combination of *in vitro*, *in silico* and *ex vivo* studies, we demonstrate that
455 co-expression of HSD11B1 with AKR1C3 modulates peripheral biosynthesis of 11KT, first, by competing

456 with AKR1C3 for the substrate 11KA4, and, second, by converting much of the resulting 11KT to the
457 less potent androgen 11OHT. We demonstrated that inhibition of HSD11B1 results in significantly
458 increased 11KT biosynthesis as shown by us *in vitro*, *in silico*, *ex vivo* and in a phase 2a study comparing
459 the effects of 35 days of treatment with the selective HSD11B1 inhibitor AZD4017 to placebo
460 treatment. Our data show that HSD11B1 inhibition does not only alter local, adipose tissue-specific
461 11KT concentrations, but also systemic levels, thus emphasising that peripheral tissues expressing
462 AKR1C3 are essential for 11KT biosynthesis (13). Collectively, our findings show that under normal
463 circumstances HSD11B1 plays an important novel role in preventing 11KT accumulation, in addition to
464 its well-known role in local glucocorticoid activation.
465 Our findings are of immediate clinical relevance, particularly in women, where circulating
466 concentrations of 11KT are similar to testosterone concentrations (3, 6, 66, 67). Therefore, increasing
467 11KT due to HSD11B1 inhibition markedly increases the total circulating pool of active androgens in
468 women. This increase in androgen load is significant given that 11KT has shown functional activity
469 comparable to testosterone (5, 62, 68) and increased circulating androgens have been linked to a
470 significantly greater risk of type 2 diabetes in women (43). Moreover, there is growing evidence that
471 androgens drive the risk of common metabolic disorders, including type 2 diabetes, hypertension,
472 cardiovascular disease and MASLD (15, 43, 69–72, 44, 46–52), in women with PCOS where androgen
473 excess is a hallmark (72). Notably, O'Reilly et. al. have previously shown that local AKR1C3-mediated
474 androgen activation in adipose tissue drives lipotoxicity in women with PCOS (15). They propose a
475 vicious cycle in which increased androgen generation in adipose tissue results in lipid accumulation,
476 increased fat mass and as a result systemic insulin resistance. This cycle is completed by the insulin-
477 induced stimulation of AKR1C3 expression in adipose, leading to increased androgen activation. Given
478 that 11KA4 is the preferred substrate for AKR1C3, increased insulin-induced AKR1C3 expression would
479 therefore lead to significantly more 11KT being produced, which would be further increased by
480 HSD11B1 inhibition (16, 17, 73).
481 Our finding of increased 11KT biosynthesis to clinically highly relevant concentrations occurring after
482 HSD11B1 inhibition therefore needs to be taken into account when considering HSD11B1 inhibition as

483 treatment for type 2 diabetes or metabolic syndrome in women, as the beneficial effects of reduced
484 local glucocorticoid activation could be offset by opposing metabolic effects due to increased 11KT
485 concentrations and AR signalling. This is highly relevant for the recently proposed use of HSD11B1
486 inhibitors in ameliorating the metabolically adverse consequences of mild autonomous cortisol excess
487 (MACS) due to adrenal adenomas (74) as affected patients are predominantly female (75).
488 Notably, quantification of AKR1C3 and HSD11B1 expression levels in subcutaneous and omental
489 adipose tissue revealed a degree of interpersonal variation. Our computational simulations revealed
490 that variations in the relative, as well as the absolute expression levels of HSD11B1 and AKR1C3 would
491 result in individual differences in the amount of 11KT produced as well as the magnitude of change
492 upon HSD11B1 inhibition. Indeed, this biological variation was reflected in both the *ex vivo* adipose
493 tissue conversion data and the serum concentrations of 11KT before and after administration of
494 AZD4017 in individuals with type 2 diabetes. Our simulations suggest that when considering 11KT
495 biosynthesis, individuals with higher HSD11B1 expression relative to AKR1C3 would be less responsive
496 to partial HSD11B1 inhibition. However, if HSD11B1 activity is completely abolished by inhibition then
497 the amount of 11KT produced is dependent of the absolute levels of AKR1C3 expressed. Increased
498 11KT concentrations are therefore not solely dependent on the inhibition of HSD11B1, but also on the
499 amount of AKR1C3 expressed. Notably, AKR1C3 expression correlates with BMI in subcutaneous, but
500 not omental, adipose tissue and its expression is upregulated by insulin (14, 15, 17). Women with
501 insulin resistance and obesity due to metabolic syndrome are therefore likely to have high expression
502 levels of AKR1C3 (14, 15), which would result in greater increases in 11KT upon inhibition of HSD11B1.
503 Thus, while such women may benefit from the local reduction of glucocorticoid activation by HSD11B1
504 inhibition in adipose tissue, they may be primed to generate more 11KT. Indeed, we noted that the
505 expression of AKR1C3 was higher than that of HSD11B1 in adipose tissue obtained from women with
506 obesity undergoing elective bariatric surgery. As a result, the conversion of 11KA4 yielded more 11KT
507 and 11OHT combined (both requiring AKR1C3 activity) than 11OHA4. In subcutaneous adipose tissue,
508 which had a lower HSD11B1:AKR1C3 ratio compared to omental adipose tissue, 11OHT was the most
509 abundant product, demonstrating effective conversion of 11KA4 to 11KT by AKR1C3 and subsequent

510 conversion of 11KT to 11OHT by HSD11B1. Similarly, we noted that in our clinical cohort, which
511 consisted of individuals with type 2 diabetes (BMI mostly in the obese range), the mean circulating
512 11OHT concentration was ≥2-fold higher than previously reported for healthy individuals thus
513 suggesting high peripheral AKR1C3 expression (3). Interestingly, a previous *ex vivo* study found that
514 androgen exposure upregulates HSD11B1 expression in adipose tissue (76) emphasising that
515 inactivation of 11-oxygenated androgens by HSD11B1 might be a protective mechanism, that no longer
516 suffices once AKR1C3 is significantly upregulated, e.g. in the context of PCOS (15).
517 Increased 11KT concentrations following HSD11B1 inhibition are unlikely to be a concern in men as the
518 metabolic effects of androgens are sexually dimorphic. In men, reduced androgen concentrations are
519 associated with adverse metabolic consequences, including insulin resistance, type 2 diabetes and
520 metabolic syndrome, and as such increased 11KT levels have the potential to be beneficial (43, 71,
521 77). Glucocorticoids are, however, also known to have sexually dimorphic effects, which are further
522 complicated by crosstalk between glucocorticoids and androgens (78–80). Unfortunately, the vast
523 majority of HSD11B1 inhibitor clinical studies did not report sex-specific outcomes for HSD11B1
524 inhibition (34–38). Larger sex-specific studies are therefore needed to fully assess the benefits of
525 HSD11B1 inhibition in relation to metabolic conditions, while taking into account potential opposing
526 androgenic effects in women, resulting from increased 11KT.
527 One recent study by Hardy *et al.* investigated the effects of HSD11B1 inhibition in women with obesity
528 and Idiopathic Intracranial Hypertension (41). Twice daily administration of 400 mg AZD4017 for 12
529 weeks had no effect on fasting glucose, fasting insulin, insulin resistance or HbA1c, in agreement with
530 our hypothesis that androgenic effects may counter beneficial metabolic effects of reduced
531 glucocorticoid concentrations. Furthermore, this study found no effect of HSD11B1 inhibition on
532 adipose or bone composition, but did report reduced cholesterol and increased HDL with HSD11B1
533 inhibition suggesting that women do exhibit some cardioprotective responses to HSD11B1 inhibition.
534 Importantly, Hardy *et al*. also reported increased lean muscle mass with HSD11B1 inhibition, which
535 correlated with increased testosterone and 11-oxygenated androgen precursors (11OHA4 and 11KA4)
536 levels; however, they did not report 11KT concentrations.

537 Increased adrenal output of 11OHA4 is not unexpected with HSD11B1 inhibition, which leads to
538 reduced negative feedback on the HPA-axis, increased ACTH levels and increased adrenal output of
539 cortisol and adrenal androgen precursors (41). While we did not observe increased serum 11OHA4
540 concentrations in the current study, we cannot exclude that increased adrenal output of this precursor
541 contributed to the observed increase in 11KT biosynthesis. In fact, this is likely the case as circulating
542 11OHA4 concentrations were not reduced despite inhibition of HSD11B1 and the resulting significant
543 decrease in the 11OHA4/11KA4 ratio. Furthermore, the original clinical trial observed a significant
544 increase in serum DHEAS, a marker of adrenal C19 steroid biosynthesis, thus confirming the stimulation
545 of adrenal steroidogenesis (40). Despite the potential increase in adrenal 11OHA4 biosynthesis, our *in*
546 *vitro*, *ex vivo* and *in silico* data unequivocally show that HSD11B1 modulates the peripheral
547 biosynthesis of 11KT and that inhibition of HSD11B1 results in increased peripheral 11KT production
548 irrespective of adrenal 11OHA4 output.
549 This study highlights that HSD11B1 inhibition may not be as effective as previously anticipated for the
550 treatment of metabolic conditions in women due to the concomitant increase in the active androgen
551 pool. However, the current data does not call into question the safety or efficacy of HSD11B1 inhibitors
552 such as AZD4017, which has been shown to be well tolerated (39–41, 63, 81), but rather highlights
553 that the condition targeted by the use of HSD11B1 inhibitors needs to be carefully considered. To date,
554 AZD4017 has shown promise in the treatment of Idiopathic Intracranial Hypertension and wound
555 healing in adults with type 2 diabetes, thus warranting further studies (40, 41). It may also be
556 interesting to consider HSD11B1 inhibition in oophorectomized women. In this setting, the increased
557 biosynthesis of 11KT due to HSD11B1 inhibition may be beneficial in offsetting the androgen deficiency
558 due to oophorectomy, while reduced local glucocorticoid activation has the potential to protect
559 against glucocorticoid induced osteoporosis, especially against the backdrop of reduced estrogen
560 biosynthesis (82–84).
561 While the current study focusses on the regulation of 11-ketotestosterone biosynthesis by HSD11B1
562 in adipose tissue, HSD11B1 is also abundantly expressed in liver and as such the hepatic conversion of

563 11KA4 to 11OHA4 and 11KT to 11OHT may also regulate systemic 11KT levels, with inhibition of hepatic
564 HSD11B1 by AZD4017 contributing to the observed increase in 11KT levels (18, 19).
565 In summary, our findings indicate that HSD11B1 plays an essential role in modulating the amount of
566 11KT produced by AKR1C3 expressed in adipose tissue. As a result, inhibition of HSD11B1 does not just
567 reduce local glucocorticoid activation, but also alters the biosynthesis of the potent 11-oxygenated
568 androgen 11KT. In women, the significant increase in 11KT concentrations may have metabolically
569 opposing effects that attenuate the beneficial reduction of glucocorticoid activation in metabolic
570 tissue. It is therefore imperative that future HSD11B1 inhibitor studies consider both the glucocorticoid
571 and androgen pools and that sex-specific effects are systematically investigated and considered in the
572 design of future studies.
573
574 **Data Availability**
575 The data that support the findings of this study are available in the results and/or supplementary
576 material of this article. The computational model is available in SBML format upon request.
577
578 **Conflict-of-interest**
579 The authors declare no conflicts of interest
580
581 **Author contributions**
582 KHS, WA and LS were responsible for study concept and design. LS and IO conducted experiments. JS
583 performed all computational modelling. LS, IO, JS, LCG, AET, and KHS analysed data. AJC and RS
584 provided human adipose tissue. AT, RA and AF provided serum and urine from a phase 2b pilot trial
585 with AZD4017. AET and LCG conducted the analysis of clinical samples by LC-MS/MS and GC-MS,
586 respectively. KHS, LS and IO drafted the manuscript. WA, AT and JS critically reviewed the manuscript.
587 All authors reviewed and approved the final version of the manuscript. KS and WA obtained funding.
588 These authors contributed equally: LS and IO. LS was selected as the first of the two authors as she
589 was involved in the conceptualisation of the study.

590 **Funding**

591 This work has been supported by the National Research Foundation of South Africa (Grant Number
592 132503, to KHS); the Academy of Medical Sciences UK (Newton Advanced Fellowship NAF004\1002,
593 to KHS); the Wellcome Trust (Investigator Grant WT209492/Z/17/Z, to WA); a Medical Research
594 Council Confidence in Concept Award to AT (MC_PC_15046); and a SARChI DST/NRF grant (82813, to
595 JS).

596 **References**

597 1. Pretorius, E., Arlt, W., and Storbeck, K.-H. (2017) A new dawn for androgens: Novel lessons
598 from 11-oxygenated C19 steroids. *Mol. Cell. Endocrinol.* **441**, 76–85
599 2. Turcu, A. F., Rege, J., Auchus, R. J., and Rainey, W. E. (2020) 11-Oxygenated androgens in
600 health and disease. *Nat. Rev. Endocrinol.* **16**, 284–296
601 3. Schiffer, L., Kempegowda, P., Sitch, A. J., Adaway, J. E., Shaheen, F., Ebbehoj, A., Singh, S.,
602 McTaggart, M. P., O'Reilly, M. W., Prete, A., Hawley, J. M., Keevil, B. G., Bancos, I., Taylor, A.
603 E., and Arlt, W. (2023) Classic and 11-oxygenated androgens in serum and saliva across
604 adulthood: a cross-sectional study analyzing the impact of age, body mass index, and diurnal
605 and menstrual cycle variation. *Eur. J. Endocrinol.* **188**, 1–15
606 4. Storbeck, K.-H. and O'Reilly, M. W. (2023) The clinical and biochemical significance of 11-
607 oxygenated androgens in human health and disease. *Eur. J. Endocrinol.* **188**, R98–R109
608 5. Pretorius, E., Africander, D. J., Vlok, M., Perkins, M. S., Quanson, J. L., and Storbeck, K.-H.
609 (2016) 11-ketotestosterone and 11-ketodihydrotestosterone in castration resistant prostate
610 cancer: potent androgens which can no longer be ignored. *PLoS One* **11**, e0159867
611 6. Nanba, A. T., Rege, J., Ren, J., Auchus, R. J., Rainey, W. E., and Turcu, A. F. (2019) 11-
612 Oxygenated C19 Steroids Do Not Decline with Age in Women. *J. Clin. Endocrinol. Metab.* **104**,
613 2615–2622
614 7. Skiba, M. A., Bell, R. J., Islam, R. M., Handelsman, D. J., Desai, R., and Davis, S. R. (2019)
615 Androgens During the Reproductive Years: What Is Normal for Women? *J Clin Endocrinol*
616 *Metab* **104**, 5382–5392
617 8. O'Reilly, M. W., Kempegowda, P., Jenkinson, C., Taylor, A. E., Quanson, J. L., Storbeck, K.-H. H.,
618 and Arlt, W. (2017) 11-oxygenated C19 steroids are the predominant androgens in polycystic
619 ovary syndrome. *J. Clin. Endocrinol. Metab.* **102**, 840–848
620 9. Turcu, A. F., Nanba, A. T., Chomic, R., Upadhyay, S. K., Giordano, T. J., Shields, J. J., Merke, D.
621 P., Rainey, W. E., and Auchus, R. J. (2016) Adrenal-derived 11-oxygenated 19-carbon steroids
622 are the dominant androgens in classic 21-hydroxylase deficiency. *Eur. J. Endocrinol.* **174**, 601–

623 609

624 10. Nowotny, H. F., Braun, L., Vogel, F., Bidlingmaier, M., Reincke, M., Tschaidse, L., Auer, M. K.,
625 Lottspeich, C., Wudy, S. A., Hartmann, M. F., Hawley, J., Adaway, J. E., Keevil, B., Schilbach, K.,
626 and Reisch, N. (2022) 11-Oxygenated C19 steroids are the predominant androgens
627 responsible for hyperandrogenemia in Cushing's disease. *Eur. J. Endocrinol.* **187**, 663–673

628 11. Storbeck, K.-H., Bloem, L. M., Africander, D. J., Schloms, L., Swart, P., and Swart, A. C. (2013)
629 11β-hydroxydihydrotestosterone and 11-ketodihydrotestosterone, novel C19 steroids with
630 androgenic activity: a putative role in castration resistant prostate cancer? *Mol. Cell.*
631 *Endocrinol.* **377**, 135–146

632 12. Snaterse, G., van Dessel, L. F., van Riet, J., Taylor, A. E., van der Vlugt-Daane, M., Hamberg, P.,
633 de Wit, R., Visser, J. A., Arlt, W., Lolkema, M. P., and Hofland, J. (2021) 11-Ketotestosterone is
634 the predominant active androgen in prostate cancer patients after castration. *JCI Insight* **6**,
635 e148507

636 13. Storbeck, K.-H. (2022) A commentary on the origins of 11-ketotestosterone. *Eur J Endocrinol*
637 **187**, C5-8

638 14. Quinkler, M., Sinha, B., Tomlinson, J. W., Bujalska, I. J., Stewart, P. M., and Arlt, W. (2004)
639 Androgen generation in adipose tissue in women with simple obesity - A site-specific role for
640 17β-hydroxysteroid dehydrogenase type 5. *J. Endocrinol.* **183**, 331–342

641 15. O'Reilly, M. W., Kempegowda, P., Walsh, M., Taylor, A. E., Manolopoulos, K. N., Allwood, J.
642 W., Semple, R. K., Hebenstreit, D., Dunn, W. B., Tomlinson, J. W., Arlt, W., Reilly, M. W. O.,
643 Manolopoulos, N., and Warwick, B. (2017) AKR1C3-Mediated Adipose Androgen Generation
644 Drives Lipotoxicity in Women With Polycystic Ovary Syndrome. *J Clin Endocrinol Metab* **102**,
645 3327–3339

646 16. Barnard, M., Quanson, J. L., Mostaghel, E., Pretorius, E., Snoep, J. L., and Storbeck, K.-H.
647 (2018) 11-Oxygenated androgen precursors are the preferred substrates for aldo-keto
648 reductase 1C3 (AKR1C3): Implications for castration resistant prostate cancer. *J. Steroid*
649 *Biochem. Mol. Biol.* **183**, 192–201

650 17. Paulukinas, R. D., Mesaros, C. A., and Penning, T. M. (2022) Conversion of Classical and 11-
651 oxygenated Androgens by Insulin Induced AKR1C3 in a Model of Human PCOS Adipocytes.
652 *Endocrinology* **163**, bqac068
653 18. Tomlinson, J. W., Walker, E. A., Bujalska, I. J., Draper, N., Lavery, G. G., Cooper, M. S.,
654 Hewison, M., and Stewart, P. M. (2004) 11β-Hydroxysteroid Dehydrogenase Type 1: A Tissue-
655 Specific Regulator of Glucocorticoid Response. *Endocr. Rev.* **25**, 831–866
656 19. Gathercole, L. L., Lavery, G. G., Morgan, S. A., Cooper, M. S., Sinclair, A. J., Tomlinson, J. W.,
657 and Stewart, P. M. (2013) 11β-Hydroxysteroid Dehydrogenase 1: Translational and
658 Therapeutic Aspects. *Endocr. Rev.* **34**, 525–555
659 20. Gent, R., du Toit, T., Bloem, L. M., and Swart, A. C. (2019) The 11β-hydroxysteroid
660 dehydrogenase isoforms: pivotal catalytic activities yield potent C11-oxy C 19 steroids with
661 11βHSD2 favouring 11-ketotestosterone, 11-ketoandrostenedione and 11-ketoprogesterone
662 biosynthesis. *J. Steroid Biochem. Mol. Biol.* **189**, 116–126
663 21. Morgan, S. A., McCabe, E. L., Gathercole, L. L., Hassan-Smith, Z. K., Larner, D. P., Bujalska, I. J.,
664 Stewart, P. M., Tomlinson, J. W., and Lavery, G. G. (2014) 11β-HSD1 is the major regulator of
665 the tissue-specific effects of circulating glucocorticoid excess. *Proc. Natl. Acad. Sci. U. S. A.*
666 **111**, E2482–E2491
667 22. Gregory, S., Hill, D., Grey, B., Ketelbey, W., Miller, T., Muniz-Terrera, G., and Ritchie, C. W.
668 (2020) 11β-hydroxysteroid dehydrogenase type 1 inhibitor use in human disease-a systematic
669 review and narrative synthesis. *Metabolism.* **108**, 154246
670 23. Tiganescu, A., Hupe, M., Uchida, Y., Mauro, T., Elias, P. M., and Holleran, W. M. (2018) Topical
671 11β-Hydroxysteroid Dehydrogenase Type 1 Inhibition Corrects Cutaneous Features of
672 Systemic Glucocorticoid Excess in Female Mice. *Endocrinology* **159**, 547–556
673 24. Doig, C. L., Fletcher, R. S., Morgan, S. A., McCabe, E. L., Larner, D. P., Tomlinson, J. W., Stewart,
674 P. M., Philp, A., and Lavery, G. G. (2017) 11β-HSD1 Modulates the Set Point of Brown Adipose
675 Tissue Response to Glucocorticoids in Male Mice. *Endocrinology* **158**, 1964–1976
676 25. Masuzaki, H., Paterson, J., Shinyama, H., Morton, N. M., Mullins, J. J., Seckl, J. R., and Flier, J. S.

677 (2001) A transgenic model of visceral obesity and the metabolic syndrome. *Science (80-.).*
678 **294**, 2166–2170
679 26. Masuzaki, H., Yamamoto, H., Kenyon, C. J., Elmquist, J. K., Morton, N. M., Paterson, J. M.,
680 Shinyama, H., Sharp, M. G. F., Fleming, S., Mullins, J. J., Seckl, J. R., and Flier, J. S. (2003)
681 Transgenic amplification of glucocorticoid action in adipose tissue causes high blood pressure
682 in mice. *J. Clin. Invest.* **112**, 83–90
683 27. Kotelevtsev, Y., Holmes, M. C., Burchell, A., Houston, P. M., Schmoll, D., Jamieson, P., Best, R.,
684 Brown, R., Edwards, C. R., Seckl, J. R., and Mullins, J. J. (1997) 11beta-hydroxysteroid
685 dehydrogenase type 1 knockout mice show attenuated glucocorticoid-inducible responses
686 and resist hyperglycemia on obesity or stress. *Proc. Natl. Acad. Sci. U. S. A.* **94**, 14924–14929
687 28. Hermanowski-Vosatka, A., Balkovec, J. M., Cheng, K., Chen, H. Y., Hernandez, M., Koo, G. C.,
688 Le Grand, C. B., Li, Z., Metzger, J. M., Mundt, S. S., Noonan, H., Nunes, C. N., Olson, S. H.,
689 Pikounis, B., Ren, N., Robertson, N., Schaeffer, J. M., Shah, K., Springer, M. S., Strack, A. M.,
690 Strowski, M., Wu, K., Wu, T. J., Xiao, J., Zhang, B. B., Wright, S. D., and Thieringer, R. (2005)
691 11β-HSD1 inhibition ameliorates metabolic syndrome and prevents progression of
692 atherosclerosis in mice. *J. Exp. Med.* **202**, 517–527
693 29. Morgan, S. A., Gathercole, L. L., Hassan-Smith, Z. K., Tomlinson, J., Stewart, P. M., and Lavery,
694 G. G. (2022) 11β-HSD1 contributes to age-related metabolic decline in male mice. *J.*
695 *Endocrinol.* **255**, 117–129
696 30. Rege, J., Garber, S., Conley, A. J., Elsey, R. M., Turcu, A. F., Auchus, R. J., and Rainey, W. E.
697 (2019) Circulating 11-oxygenated androgens across species. *J. Steroid Biochem. Mol. Biol.* **190**,
698 242–249
699 31. Walker, B. R., Connacher, A. A., Lindsay, R. M., Webb, D. J., and Edwards, C. R. W. (1995)
700 Carbenoxolone increases hepatic insulin sensitivity in man: a novel role for 11-oxosteroid
701 reductase in enhancing glucocorticoid receptor activation. *J. Clin. Endocrinol. Metab.* **80**,
702 3155–3159
703 32. Andrews, R. C., Rooyackers, O., and Walker, B. R. (2003) Effects of the 11 beta-hydroxysteroid

704 dehydrogenase inhibitor carbenoxolone on insulin sensitivity in men with type 2 diabetes. *J.*
705 *Clin. Endocrinol. Metab.* **88**, 285–291
706 33. Sandeep, T. C., Andrew, R., Homer, N. Z. M., Andrews, R. C., Smith, K., and Walker, B. R. (2005)
707 Increased in vivo regeneration of cortisol in adipose tissue in human obesity and effects of the
708 11beta-hydroxysteroid dehydrogenase type 1 inhibitor carbenoxolone. *Diabetes* **54**, 872–879
709 34. Rosenstock, J., Banarer, S., Fonseca, V. A., Inzucchi, S. E., William, S., Wenqing, Y., Hollis, G.,
710 Flores, R., Levy, R., Williams, W. V., Seckl, J. R., and Huber, R. (2010) The 11-beta-
711 hydroxysteroid dehydrogenase type 1 inhibitor INCB13739 improves hyperglycemia in
712 patients with type 2 diabetes inadequately controlled by metformin monotherapy. *Diabetes*
713 *Care* **33**, 1516–1522
714 35. Feig, P. U., Shah, S., Hermanowski-Vosatka, A., Plotkin, D., Springer, M. S., Donahue, S., Thach,
715 C., Klein, E. J., Lai, E., and Kaufman, K. D. (2011) Effects of an 11β-hydroxysteroid
716 dehydrogenase type 1 inhibitor, MK-0916, in patients with type 2 diabetes mellitus and
717 metabolic syndrome. *Diabetes. Obes. Metab.* **13**, 498–504
718 36. Shah, S., Hermanowski-Vosatka, A., Gibson, K., Ruck, R. A., Jia, G., Zhang, J., Hwang, P. M. T.,
719 Ryan, N. W., Langdon, R. B., and Feig, P. U. (2011) Efficacy and safety of the selective 11β-
720 HSD-1 inhibitors MK-0736 and MK-0916 in overweight and obese patients with hypertension.
721 *J. Am. Soc. Hypertens.* **5**, 166–176
722 37. Heise, T., Morrow, L., Hompesch, M., Häring, H. U., Kapitza, C., Abt, M., Ramsauer, M.,
723 Magnone, M. C., and Fuerst-Recktenwald, S. (2014) Safety, efficacy and weight effect of two
724 11β-HSD1 inhibitors in metformin-treated patients with type 2 diabetes. *Diabetes. Obes.*
725 *Metab.* **16**, 1070–1077
726 38. Yadav, Y., Dunagan, K., Khot, R., Venkatesh, S. K., Port, J., Galderisi, A., Cobelli, C., Wegner, C.,
727 Basu, A., Carter, R., and Basu, R. (2022) Inhibition of 11β-Hydroxysteroid dehydrogenase-1
728 with AZD4017 in patients with nonalcoholic steatohepatitis or nonalcoholic fatty liver disease:
729 A randomized, double-blind, placebo-controlled, phase II study. *Diabetes. Obes. Metab.* **24**,
730 881–890

731 39. Abbas, A., Schini, M., Ainsworth, G., Brown, S. R., Oughton, J., Crowley, R. K., Cooper, M. S.,
732 Fairclough, R. J., Eastell, R., and Stewart, P. M. (2022) Effect of AZD4017, a Selective 11β-HSD1
733 Inhibitor, on Bone Turnover Markers in Postmenopausal Osteopenia. *J. Clin. Endocrinol.*
734 *Metab.* **107**, 2026–2035
735 40. Ajjan, R. A., Hensor, E. M. A., Del Galdo, F., Shams, K., Abbas, A., Fairclough, R. J., Webber, L.,
736 Pegg, L., Freeman, A., Taylor, A. E., Arlt, W., Morgan, A. W., Tahrani, A. A., Stewart, P. M.,
737 Russell, D. A., and Tiganescu, A. (2022) Oral 11β-HSD1 inhibitor AZD4017 improves wound
738 healing and skin integrity in adults with type 2 diabetes mellitus: a pilot randomized
739 controlled trial. *Eur. J. Endocrinol.* **186**, 441–455
740 41. Hardy, R. S., Botfield, H., Markey, K., Mitchell, J. L., Alimajstorovic, Z., Westgate, C. S. J.,
741 Sagmeister, M., Fairclough, R. J., Ottridge, R. S., Yiangou, A., Storbeck, K. H. H., Taylor, A. E.,
742 Gilligan, L. C., Arlt, W., Stewart, P. M., Tomlinson, J. W., Mollan, S. P., Lavery, G. G., and
743 Sinclair, A. J. (2021) 11βHSD1 Inhibition with AZD4017 Improves Lipid Profiles and Lean
744 Muscle Mass in Idiopathic Intracranial Hypertension. *J. Clin. Endocrinol. Metab.* **106**, 174–187
745 42. Bianzano, S., Nordaby, M., Plum-Mörschel, L., Peil, B., and Heise, T. (2023) Safety, tolerability,
746 pharmacodynamics and pharmacokinetics following once-daily doses of BI 187004, an
747 inhibitor of 11 beta-hydroxysteroid dehydrogenase-1, over 28 days in patients with type 2
748 diabetes mellitus and overweight or obesity. *Diabetes, Obes. Metab.* **25**, 832–843
749 43. O'Reilly, M. W., Glisic, M., Kumarendran, B., Subramanian, A., Manolopoulos, K. N., Tahrani, A.
750 A., Keerthy, D., Muka, T., Toulis, K. A., Hanif, W., Thomas, G. N., Franco, O. H., Arlt, W., and
751 Nirantharakumar, K. (2019) Serum testosterone, sex hormone-binding globulin and sex-
752 specific risk of incident type 2 diabetes in a retrospective primary care cohort. *Clin.*
753 *Endocrinol. (Oxf).* **90**, 145–154
754 44. Fauser, B. C. J. M., Tarlatzis, Fauser, Chang, Aziz, Legro, Dewailly, Franks, Balen, Bouchard,
755 Dahlgren, Devoto, Diamanti, Dunaif, Filicori, Homburg, Ibanez, Laven, Magoffin, Nestler,
756 Norman, Pasquali, Pugeat, Strauss, Tan, Taylor, Wild, Wild, Guzik, Ehrmann, and Lobo. (2004)
757 Revised 2003 consensus on diagnostic criteria and long-term health risks related to polycystic

758 ovary syndrome (PCOS). *Hum. Reprod.* **19**, 41–47

759 45. Legro, R. S., Arslanian, S. A., Ehrmann, D. A., Hoeger, K. M., Murad, M. H., Pasquali, R., and
760 Welt, C. K. (2013) Diagnosis and treatment of polycystic ovary syndrome: An endocrine
761 society clinical practice guideline. *J. Clin. Endocrinol. Metab.* **98**, 4565–4592

762 46. McCartney, C. R. and Marshall, J. C. (2016) Polycystic Ovary Syndrome. *N. Engl. J. Med.* **375**,
763 54–64

764 47. Legro, R. S., Kunselman, A. R., Dodson, W. C., and Dunaif, A. (1999) Prevalence and Predictors
765 of Risk for Type 2 Diabetes Mellitus and Impaired Glucose Tolerance in Polycystic Ovary
766 Syndrome: A Prospective, Controlled Study in 254 Affected Women. *J. Clin. Endocrinol. Metab.*
767 **84**, 165–169

768 48. Randeva, H. S., Tan, B. K., Weickert, M. O., Lois, K., Nestler, J. E., Sattar, N., and Lehnert, H.
769 (2012) Cardiometabolic Aspects of the Polycystic Ovary Syndrome. *Endocr. Rev.* **33**, 812–841

770 49. Jones, H., Sprung, V. S., Pugh, C. J. A., Daousi, C., Irwin, A., Aziz, N., Adams, V. L., Thomas, E. L.,
771 Bell, J. D., Kemp, G. J., and Cuthbertson, D. J. (2012) Polycystic ovary syndrome with
772 hyperandrogenism is characterized by an increased risk of hepatic steatosis compared to
773 nonhyperandrogenic PCOS phenotypes and healthy controls, independent of obesity and
774 insulin resistance. *J. Clin. Endocrinol. Metab.* **97**, 3709–3716

775 50. Rocha, A. L. L., Faria, L. C., Guimarães, T. C. M., Moreira, G. V., Cândido, A. L., Couto, C. A., and
776 Reis, F. M. (2017) Non-alcoholic fatty liver disease in women with polycystic ovary syndrome:
777 systematic review and meta-analysis. *J. Endocrinol. Invest.* **40**, 1279–1288

778 51. Cai, J., Wu, C. H., Zhang, Y., Wang, Y. Y., Xu, W. D., Lin, T. C., Li, S. X., Wang, L. H., Zheng, J.,
779 Sun, Y., Liu, W., and Tao, T. (2017) High-free androgen index is associated with increased risk
780 of non-alcoholic fatty liver disease in women with polycystic ovary syndrome, independent of
781 obesity and insulin resistance. *Int. J. Obes.* **41**, 1341–1347

782 52. Kumarendran, B., O'Reilly, M. W., Manolopoulos, K. N., Toulis, K. A., Gokhale, K. M., Sitch, A.
783 J., Wijeyaratne, C. N., Coomarasamy, A., Arlt, W., and Nirantharakumar, K. (2018) Polycystic
784 ovary syndrome, androgen excess, and the risk of nonalcoholic fatty liver disease in women: A

785 longitudinal study based on a United Kingdom primary care database. *PLOS Med.* **15**,
786 e1002542
787 53. Matsuura, K., Shiraishi, H., Hara, A., Sato, K., Deyashiki, Y., Ninomiya, M., and Sakai, S. (1998)
788 Identification of a Principal mRNA Species for Human 3 -Hydroxysteroid Dehydrogenase
789 Isoform (AKR1C3) That Exhibits High Prostaglandin D2 11-Ketoreductase Activity. *J. Biochem.*
790 **124**, 940–946
791 54. Pfaffl, M. W. (2001) A new mathematical model for relative quantification in real-time RT-PCR.
792 *Nucleic Acids Res.* **29**, e45
793 55. Willems, E., Leyns, L., and Vandesompele, J. (2008) Standardization of real-time PCR gene
794 expression data from independent biological replicates. *Anal. Biochem.* **379**, 127–129
795 56. Guan, H. and Yang, K. (2008) RNA isolation and real-time quantitative RT-PCR. *Methods Mol.*
796 *Biol.* **456**, 259–270
797 57. Quanson, J. L., Stander, M. A., Pretorius, E., Jenkinson, C., Taylor, A. E., and Storbeck, K.-H. H.
798 (2016) High-throughput analysis of 19 endogenous androgenic steroids by ultra-performance
799 convergence chromatography tandem mass spectrometry. *J. Chromatogr. B Anal. Technol.*
800 *Biomed. Life Sci.* **1031**, 131–138
801 58. Schiffer, L., Shaheen, F., Gilligan, L. C., Storbeck, K. H., Hawley, J. M., Keevil, B. G., Arlt, W., and
802 Taylor, A. E. (2022) Multi-steroid profiling by UHPLC-MS/MS with post-column infusion of
803 ammonium fluoride. *J. Chromatogr. B Anal. Technol. Biomed. Life Sci.* **1209**, 123413
804 59. Foster, M. A., Taylor, A. E., Hill, N. E., Bentley, C., Bishop, J., Gilligan, L. C., Shaheen, F., Bion, J.
805 F., Fallowfield, J. L., Woods, D. R., Bancos, I., Midwinter, M. M., Lord, J. M., and Arlt, W. (2020)
806 Mapping the Steroid Response to Major Trauma From Injury to Recovery: A Prospective
807 Cohort Study. *J. Clin. Endocrinol. Metab.* **105**, 925–937
808 60. Chadwick, C. A., Owen, L. J., and Keevil, B. G. (2005) Development of a method for the
809 measurement of dehydroepiandrosterone sulphate by liquid chromatography-tandem mass
810 spectrometry. *Ann. Clin. Biochem.* **42**, 468–474
811 61. Shackleton, C. H. L. (1986) Profiling steroid hormones and urinary steroids. *J Chromatogr* **379**,

812 91–156

813 62. Snaterse, G., Mies, R., van Weerden, W. M., French, P. J., Jonker, J. W., Houtsmuller, A. B., van
814 Royen, M. E., Visser, J. A., and Hofland, J. (2022) Androgen receptor mutations modulate
815 activation by 11-oxygenated androgens and glucocorticoids. *Prostate Cancer Prostatic Dis.*

816 63. Scott, J. S., Bowker, S. S., Deschoolmeester, J., Gerhardt, S., Hargreaves, D., Kilgour, E., Lloyd,
817 A., Mayers, R. M., McCoull, W., Newcombe, N. J., Ogg, D., Packer, M. J., Rees, A., Revill, J.,
818 Schofield, P., Selmi, N., Swales, J. G., and Whittamore, P. R. O. (2012) Discovery of a potent,
819 selective, and orally bioavailable acidic 11β-hydroxysteroid dehydrogenase type 1 (11β-HSD1)
820 inhibitor: discovery of 2-[(3S)-1-[5-(cyclohexylcarbamoyl)-6-propylsulfanylpyridin-2-yl]-3-
821 piperidyl]acetic acid (AZD4017). *J. Med. Chem.* **55**, 5951–5964

822 64. Barnard, L., Nikolaou, N., Louw, C., Schiffer, L., Gibson, H., Gilligan, L. C., Gangitano, E., Snoep,
823 J., Arlt, W., Tomlinson, J. W., and Storbeck, K. H. (2020) The A-ring reduction of 11-
824 ketotestosterone is efficiently catalysed by AKR1D1 and SRD5A2 but not SRD5A1. *J. Steroid*
825 *Biochem. Mol. Biol.* **202**, 105724

826 65. Tomlinson, J. W., Walker, E. A., Bujalska, I. J., Draper, N., Lavery, G. G., Cooper, M. S.,
827 Hewison, M., and Stewart, P. M. (2004) 11beta-hydroxysteroid dehydrogenase type 1: a
828 tissue-specific regulator of glucocorticoid response. *Endocr Rev* **25**, 831–866

829 66. Davio, A., Woolcock, H., Nanba, A. T., Rege, J., O'Day, P., Ren, J., Zhao, L., Ebina, H., Auchus, R.,
830 Rainey, W. E., and Turcu, A. F. (2020) Sex Differences in 11-Oxygenated Androgen Patterns
831 Across Adulthood. *J. Clin. Endocrinol. Metab.* **105**, e2921–e2929

832 67. Skiba, M. A., Bell, R. J., Islam, R. M., Handelsman, D. J., Desai, R., and Davis, S. R. (2019)
833 Androgens During the Reproductive Years: What Is Normal for Women? *J. Clin. Endocrinol.*
834 *Metab.* **104**, 5382–5392

835 68. Handelsman, D. J., Cooper, E. R., and Heather, A. K. (2022) Bioactivity of 11 keto and hydroxy
836 androgens in yeast and mammalian host cells. *J. Steroid Biochem. Mol. Biol.* **218**, 106049

837 69. Legro, R. S., Arslanian, S. A., Ehrmann, D. A., Hoeger, K. M., Murad, M. H., Pasquali, R., and
838 Welt, C. K. (2013) Diagnosis and Treatment of Polycystic Ovary Syndrome: An Endocrine

839 Society Clinical Practice Guideline. *J. Clin. Endocrinol. Metab.* **98**, 4565–4592

840 70. O'Reilly, M. W., Taylor, A. E., Crabtree, N. J., Hughes, B. A., Capper, F., Crowley, R. K., Stewart,
841 P. M., Tomlinson, J. W., and Arlt, W. (2014) Hyperandrogenemia predicts metabolic
842 phenotype in polycystic ovary syndrome: The utility of serum androstenedione. *J. Clin.*
843 *Endocrinol. Metab.* **99**, 1027–1036

844 71. Schiffer, L., Kempegowda, P., Arlt, W., and O'Reilly, M. W. (2017) MECHANISMS IN
845 ENDOCRINOLOGY: The sexually dimorphic role of androgens in human metabolic disease. *Eur.*
846 *J. Endocrinol.* **177**, R125–R143

847 72. Kempegowda, P., Melson, E., Manolopoulos, K. N., Arlt, W., and O'Reilly, M. W. (2020)
848 Implicating androgen excess in propagating metabolic disease in polycystic ovary syndrome.
849 *Ther. Adv. Endocrinol. Metab.* **11**, 2042018820934319

850 73. Paulukinas, R. D. and Penning, T. M. (2023) Insulin-Induced AKR1C3 Induces Fatty Acid
851 Synthase in a Model of Human PCOS Adipocytes. *Endocrinology* **164**, bqad033

852 74. Oda, S., Ashida, K., Uchiyama, M., Sakamoto, S., Hasuzawa, N., Nagayama, A., Wang, L.,
853 Nagata, H., Sakamoto, R., Kishimoto, J., Todaka, K., Ogawa, Y., Nakanishi, Y., and Nomura, M.
854 (2021) An Open-label Phase I/IIa Clinical Trial of 11β-HSD1 Inhibitor for Cushing's Syndrome
855 and Autonomous Cortisol Secretion. *J. Clin. Endocrinol. Metab.* **106**, E3865–E3880

856 75. Prete, A., Subramanian, A., Bancos, I., Chortis, V., Tsagarakis, S., Lang, K., Macech, M.,
857 Delivanis, D. A., Pupovac, I. D., Reimondo, G., Marina, L. V., Deutschbein, T., Balomenaki, M.,
858 O'Reilly, M. W., Gilligan, L. C., Jenkinson, C., Bednarczuk, T., Zhang, C. D., Dusek, T.,
859 Diamantopoulos, A., Asia, M., Kondracka, A., Li, D., Masjkur, J. R., Quinkler, M., Ueland, G.,
860 Dennedy, M. C., Beuschlein, F., Tabarin, A., Fassnacht, M., Ivović, M., Terzolo, M., Kastelan, D.,
861 Young, W. F., Manolopoulos, K. N., Ambroziak, U., Vassiliadi, D. A., Taylor, A. E., Sitch, A. J.,
862 Nirantharakumar, K., Arlt, W., Glöckner, S., Sinnott, R. O., Stell, A., Fragoso, M. C. B. V.,
863 Simunov, B., Cazenave, S., Haissaguerre, M., Bertherat, J., Libé, R., Kienitz, T., Eisenhofer, G.,
864 Brugger, C., Reincke, M., Riester, A., Spyroglou, A., Burger-Stritt, S., Hahner, S., Kroiss, M.,
865 Ronchi, C. L., Palimeri, S., Tsirou, I., Basile, V., Ingargiola, E., Canu, L., Mannelli, M., Ettaieb, H.,

866 Haak, H. R., Kerkhofs, T. M., Biehl, M., Feelders, R. A., Hofland, J., Hofland, L. J., Grytaas, M. A.,
867 Husebye, E. S., Zawierucha, M., Paiva, I., Sajwani, A., Sherlock, M., Crowley, R. K., Deeks, J. J.,
868 Hughes, B. A., Ivison, H. E., O'Neil, D. M., Papathomas, T. G., Ronchi, C. L., Shackleton, C. H. L.,
869 Ronchi, C. L., Sutcliffe, R. P., Guest, P., Skordilis, K., Bancos, C., Chang, A., Davidge-Pitts, C. J.,
870 Erickson, D., Natt, N., Nippoldt, T. B., Thomas, M., and Shackleton, C. H. L. (2022)
871 Cardiometabolic Disease Burden and Steroid Excretion in Benign Adrenal Tumors : A Cross-
872 Sectional Multicenter Study. *Ann. Intern. Med.* **175**, 325–334
873 76. Zhu, L., Hou, M., Sun, B., Burén, J., Zhang, L., Yi, J., Hernell, O., and Li, X. (2010) Testosterone
874 stimulates adipose tissue 11beta-hydroxysteroid dehydrogenase type 1 expression in a depot-
875 specific manner in children. *J. Clin. Endocrinol. Metab.* **95**, 3300–3308
876 77. Pivonello, R., Menafra, D., Riccio, E., Garifalos, F., Mazzella, M., De Angelis, C., and Colao, A. A.
877 (2019) Metabolic disorders and male hypogonadotropic hypogonadism. *Front. Endocrinol.*
878 *(Lausanne).* **10**, 345
879 78. Kroon, J., Pereira, A. M., and Meijer, O. C. (2020) Glucocorticoid Sexual Dimorphism in
880 Metabolism: Dissecting the Role of Sex Hormones. *Trends Endocrinol. Metab.* **31**, 357–367
881 79. Ruiz, D., Padmanabhan, V., and Sargis, R. M. (2020) Stress, sex, and sugar: Glucocorticoids and
882 sex-steroid crosstalk in the sex-specific misprogramming of metabolism. *J. Endocr. Soc.* **4**,
883 bvaa087
884 80. Kaikaew, K., Grefhorst, A., and Visser, J. A. (2021) Sex Differences in Brown Adipose Tissue
885 Function: Sex Hormones, Glucocorticoids, and Their Crosstalk. *Front. Endocrinol. (Lausanne).*
886 **12**, 357
887 81. Markey, K., Mitchell, J., Botfield, H., Ottridge, R. S., Matthews, T., Krishnan, A., Woolley, R.,
888 Westgate, C., Yiangou, A., Alimajstorovic, Z., Shah, P., Rick, C., Ives, N., Taylor, A. E., Gilligan, L.
889 C., Jenkinson, C., Arlt, W., Scotton, W., Fairclough, R. J., Singhal, R., Stewart, P. M., Tomlinson,
890 J. W., Lavery, G. G., Mollan, S. P., and Sinclair, A. J. (2020) 11β-Hydroxysteroid dehydrogenase
891 type 1 inhibition in idiopathic intracranial hypertension: a double-blind randomized controlled
892 trial. *Brain Commun.* **2**, fcz050

893 82. Shifren, J. L. (2002) Androgen deficiency in the oophorectomized woman. *Fertil. Steril.* **77**, 60–
894 62
895 83. Stanczyk, F. Z., Chaikittisilpa, S., Sriprasert, I., Rafatnia, A., Nadadur, M., and Mishell, D. R.
896 (2019) Circulating androgen levels before and after oophorectomy in premenopausal and
897 postmenopausal women. *Climacteric* **22**, 169–174
898 84. Hardy, R. S., Zhou, H., Seibel, M. J., and Cooper, M. S. (2018) Glucocorticoids and Bone:
899 Consequences of Endogenous and Exogenous Excess and Replacement Therapy. *Endocr. Rev.*
900 **39**, 519–548

901

902 **Table and figures:**

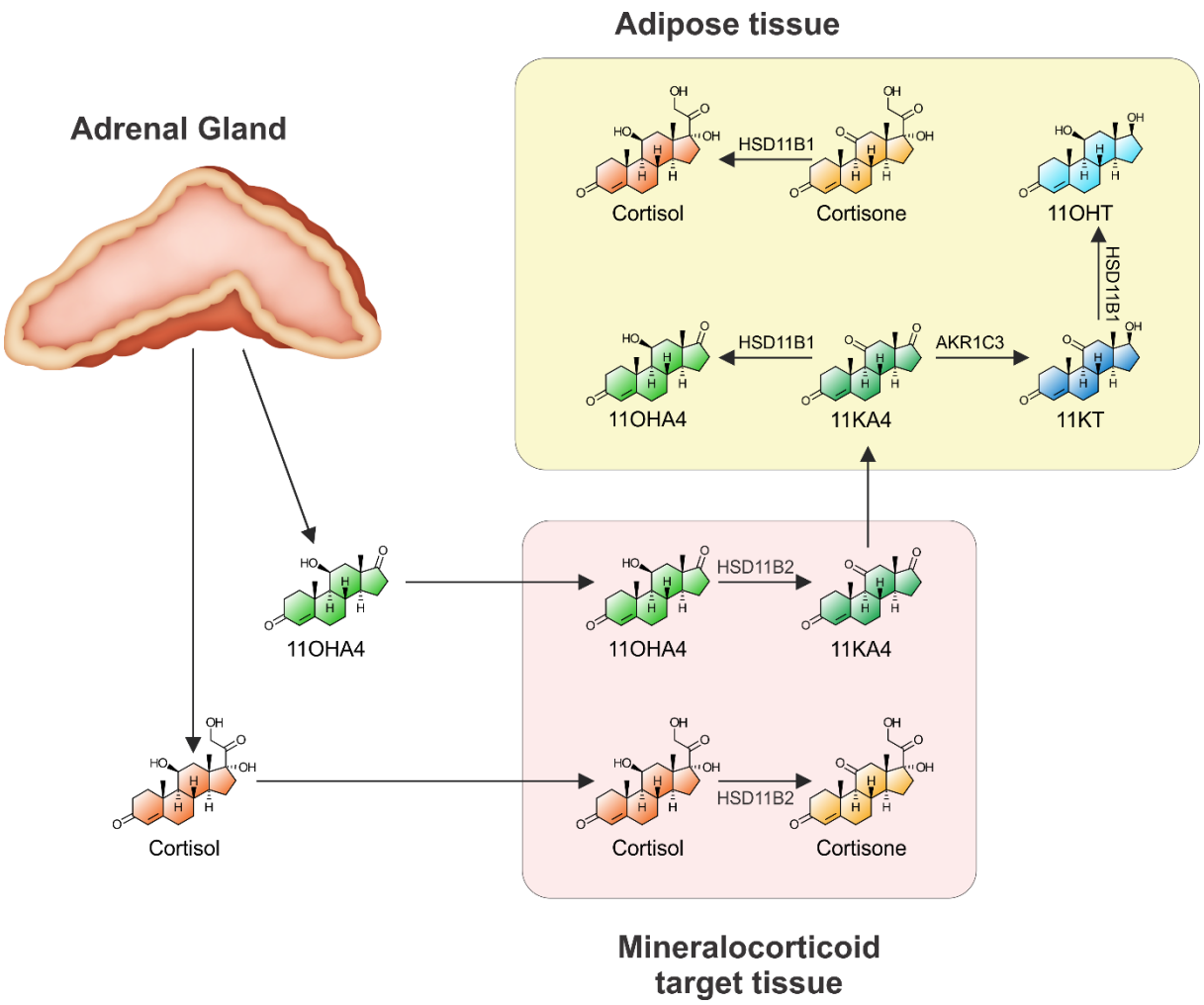

903

904 **Figure 1: Schematic showing the peripheral metabolism of cortisol and 11OHA4.** Cortisol is converted
905 to its inactive form, cortisone, by HSD11B2 expressed in mineralocorticoid target tissues. Cortisone is
906 in turn converted back to cortisol by HSD11B1 expressed in glucocorticoid target tissues (e.g., adipose).
907 Like cortisol, adrenal derived 11OHA4 is a substrate for HSD11B2, yielding 11KA4. 11KA4 is a substrate
908 for both the androgen activating enzyme AKR1C3 and HSD11B1, both of which are expressed in
909 adipose tissue. Conversion of 11KA4 to 11OHA4 by HSD11B1 prevents the conversion of 11KA4 to the
910 potent 11-oxygenated androgen, 11KT. The 11KT that is produced by AKR1C3 is also a substrate for
911 HSD11B1, yielding the substantially less active androgen, 11OHT.

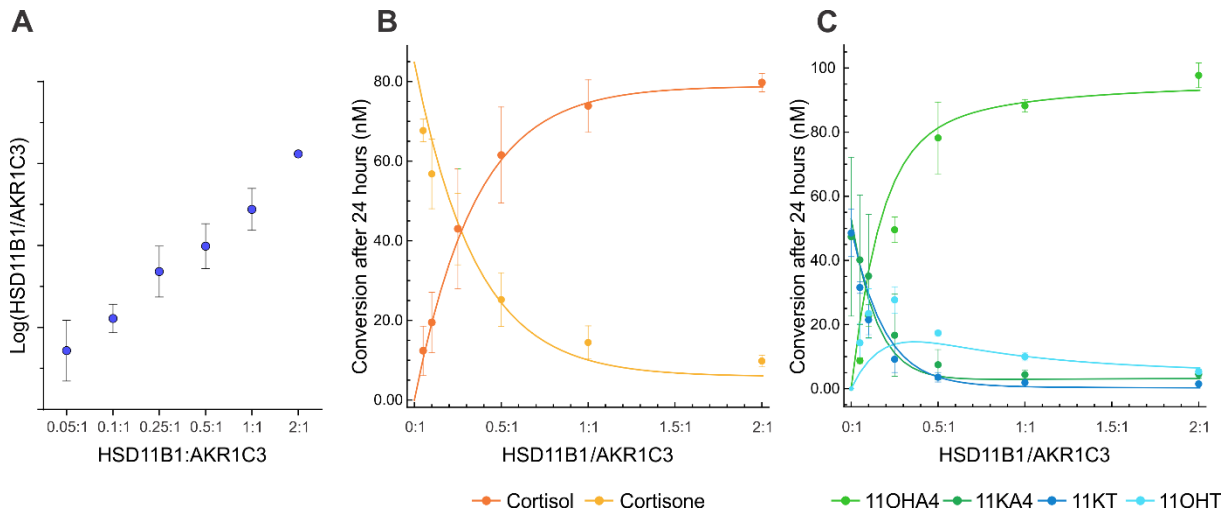

Figure 2: Increased HSD11B1:AKR1C3 ratios modulate the biosynthesis of 11KT. (A) qPCR data confirming the increase in HSD11B1 expression relative to that of AKR1C3 at the different HSD11B1:AKR1C3 ratios. **(B)** The conversion of cortisone (0.1 µM) to cortisol by increasing ratios of HSD11B1:AKR1C3 after 24 hours **(C)**. The conversion of 11KA4 (0.1 µM) to 11OHA4, 11KT and 11OHT by increasing ratios of HSD11B1:AKR1C3 after 24 hours. For **B** and **C** the experimental data from the ratio experiments are shown as points with error bars, while the computational models' predictions are shown with the solid connecting lines. All results are shown as means ± SEM of three independent experiments.

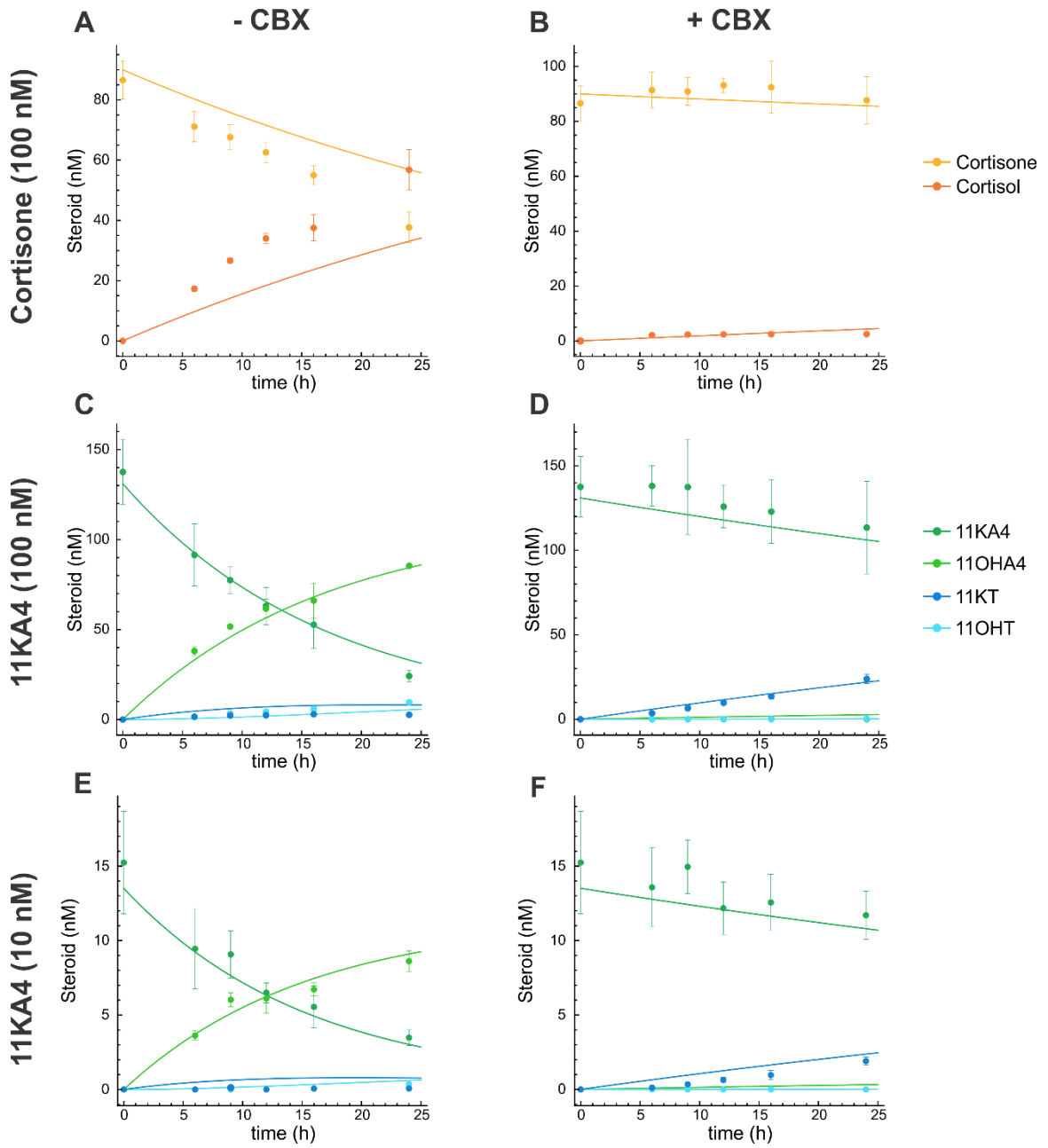

921

922 **Figure 3: Inhibition of HSD11B1 by carbenoxolone (CBX) inhibits the biosynthesis of cortisol, but**
923 **allows for increased AKR1C3-mediated production of 11KT when HSD11B1 and AKR1C3 are co-**
924 **expressed.** HEK293 cells expressing HSD11B1 and AKR1C3 were combined at a ratio of 1:1 and treated
925 with either 100 nM cortisone **(A & B)** and 100 nM 11KA4 **(C & D)** with and without CBX (10 µM) or 100
926 nM cortisone and 10 nM 11KA4 **(E & F)** with or without CBX (10 µM). The experimental data from the
927 time course experiment is shown as points with error bars, while the computational models'
928 predictions are shown with the solid lines. All results are shown as means ± SD of a single biological
929 experiment performed in triplicate. This enabled the model to predict the outcomes from one
930 experiment with the same transfection efficiency.

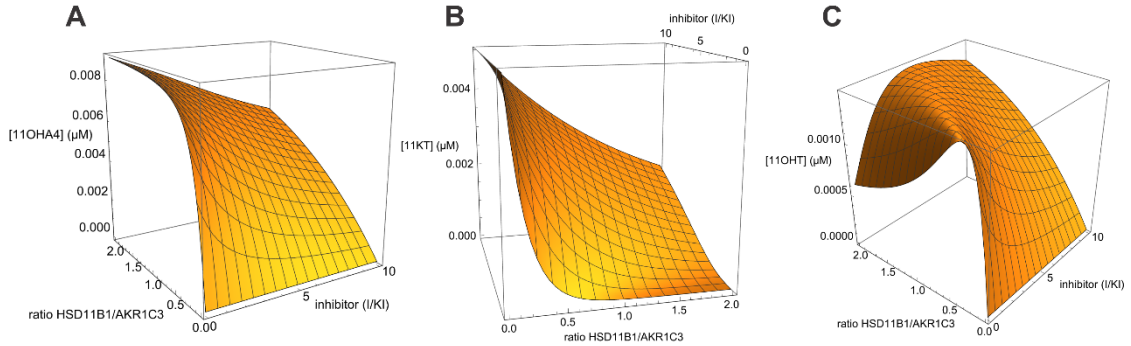

Figure 4: Computational model of the effect of varying HSD11B1:AKR1C3 ratios and different levels of HSD11B1 inhibition on the resulting concentrations of 11OHA4 (A), 11KT (B) and 11OHT (C). The model varies that ratio of HSD11B1:AKR1C3 as in Figure 2 and estimates the effect of different levels of HSD11B1 inhibition on the conversion of 10 nM 11KA4 after 24 hours as in Figures 2 and 3.

936

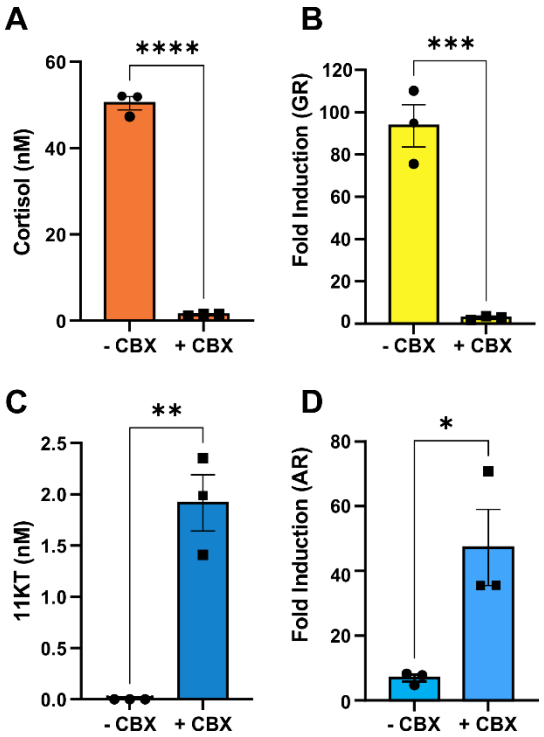

937

938 **Figure 5: Inhibition of HSD11B1 by carbenoxolone (CBX) results in decreased cortisol production (A)**
939 **and an accompanying decrease in transactivation of the glucocorticoid receptor (B), but increased**
940 **production of 11KT (C) and transactivation of the androgen receptor (D).** HEK293 cells expressing
941 HSD11B1 and AKR1C3 were combined at a ratio of 1:1 and treated with 100 nM cortisone and 10 nM
942 11KA4 with or without CBX (10 µM). After 24 hours the conditioned media was transferred to HEK293
943 cells transiently transfected with either a plasmid expressing the glucocorticoid receptor (GR) and a
944 luciferase reporter construct or a plasmid expressing the androgen receptor (AR) and the same
945 luciferase reporter construct. Luciferase was assayed after an additional 24 hour incubation and is
946 shown as the fold-induction relative to a vehicle control. All results are shown as means ± SEM of three
947 biological experiments. P values were calculated using unpaired t-tests (*P <0.05; **P<0.01;
948 ***P<0.001; ****P <0.0001).

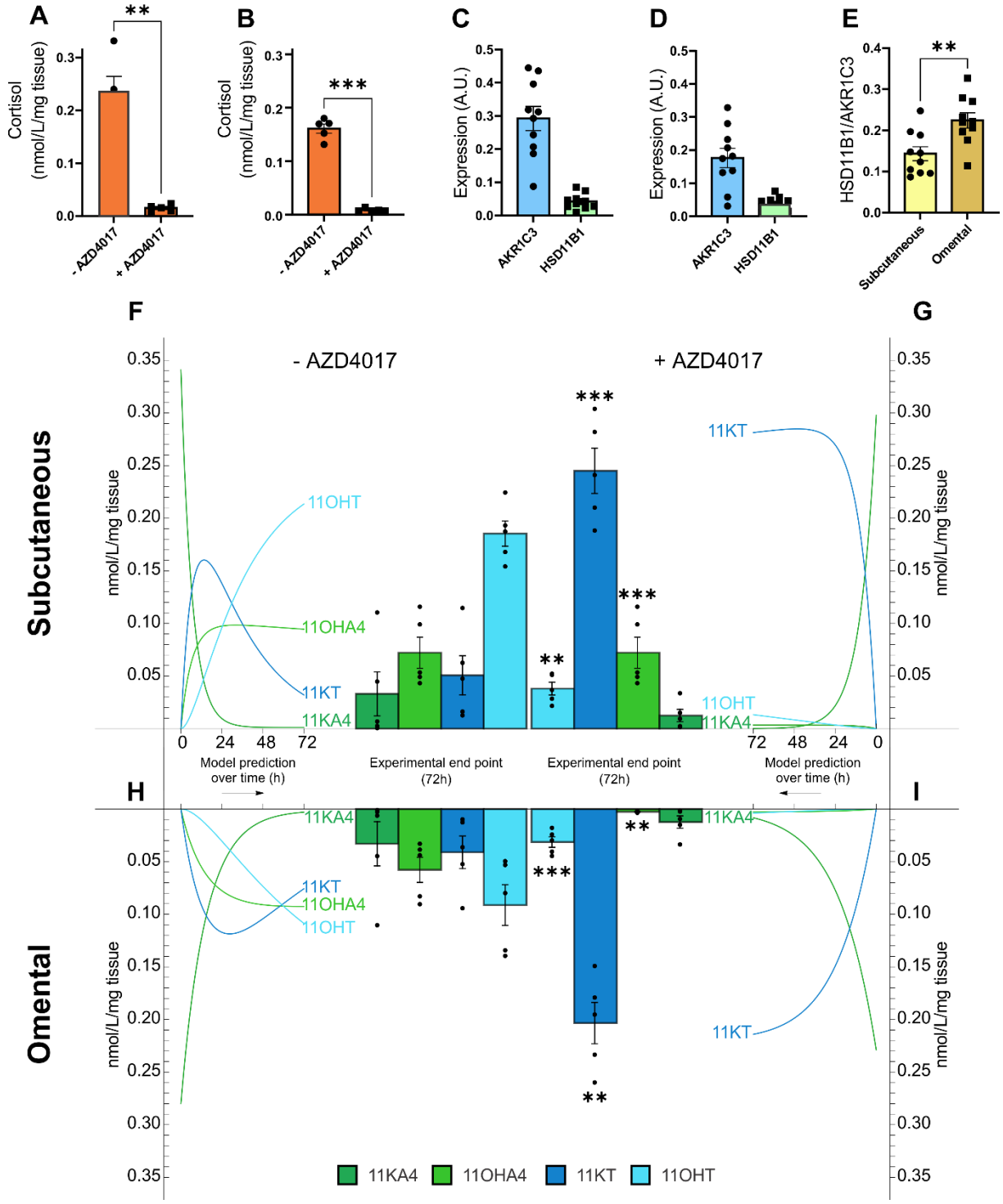

Figure 6: Inhibition of HSD11B1 by AZD4017 in human subcutaneous (A, F, G) and omental (B, H, I) adipose tissue results in the increased production of 11KT. Adipose tissue was incubated *ex vivo* with 100 nM cortisone (**A, B**) or 11KA4 (**F-I**) with or without AZD4017 (100 nM) for 72 hours. The mathematical model's prediction of the conversion over time is shown next to the experimentally determined end point data after the 72 hour incubation. Expression of AKR1C3 and HSD11B1 in subcutaneous (**C**) and omental (**D**) adipose tissue was measured by qPCR. The expression ratio of HSD11B1:AKR1C3 were determined for both adipose tissue subtypes (**E**). P values were calculated using Wilcoxon signed-rank tests (*P <0.05; **P<0.01; ***P<0.001).

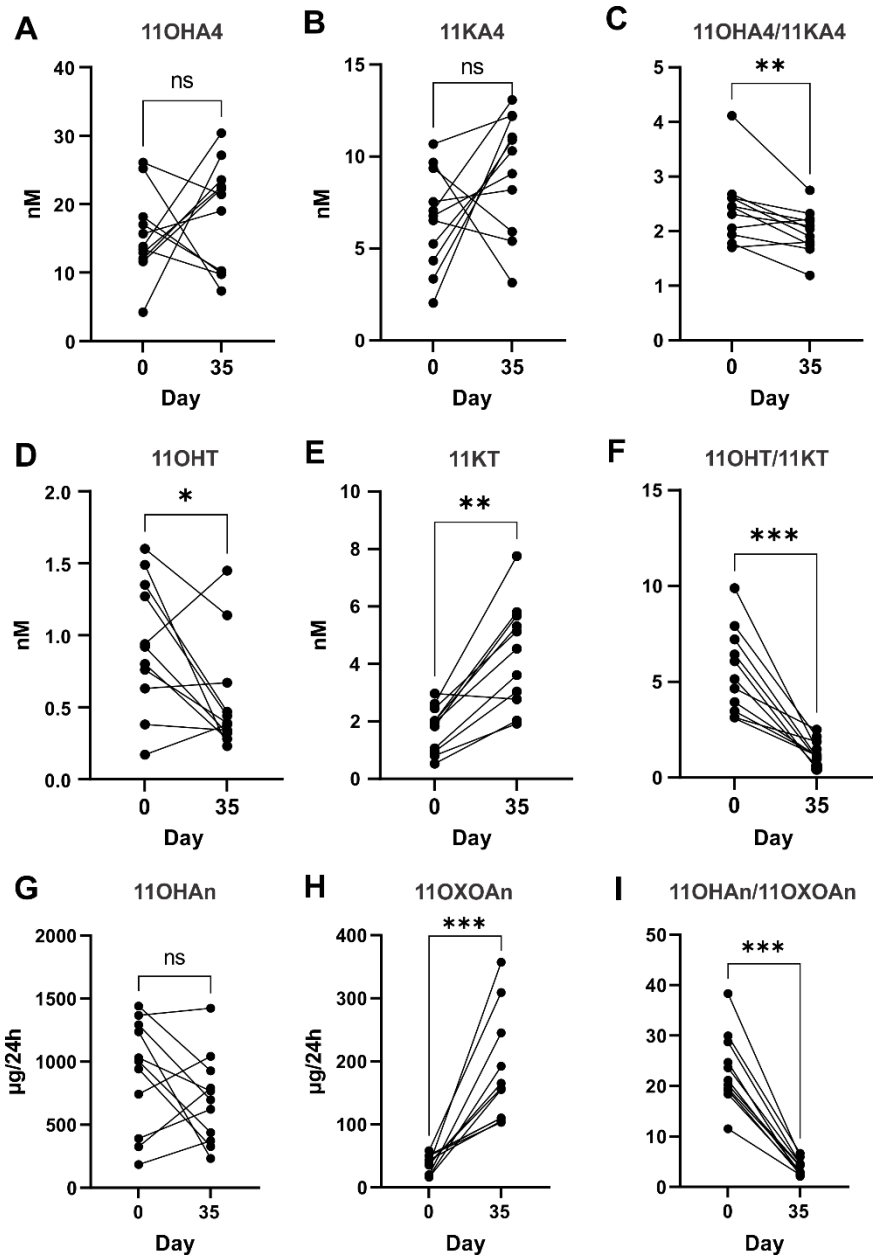

Figure 7: Inhibition of HSD11B1 by oral administration of AZD4017 (400 mg twice daily) for 35 days (n=11) changes the serum (A-F) and urinary (G-I) profile of 11-oxygenated androgens and their metabolites, with significant increases in the circulating concentration of the potent androgen 11KT. P values were calculated using Wilcoxon signed-rank tests (*P <0.05; **P<0.01; ***P<0.001). Serum concentrations of classic androgens are shown in **Supplementary Figure 7**.

964 **Table 1: Kinetic constants ($K_{m,\ app}$; $V_{max,\ app}$; V_{max}/K_m) determined for HSD11B1.**

Reaction	$K_{m,\ app\ (substrate)}$ (µM)	$K_{m,\ app\ (product)}$ (µM)	$V_{max,\ app\ (forward)}$ (µM/h)*	$V_{max,\ app\ (reverse)}$ 1/h[a] or (µM/h)[b]	V_{max}/K_m#
Cortisone -> Cortisol	0.9	-	0.12	0.01[a]	0.13
11KA4 -> 11OHA4	1	2.46	0.35	0.03[b]	0.35
11KT -> 11OHT	0.21	-	0.05	-	0.24

965 *$V_{max,\ app}$ values are dependent on transfection efficiency and differ between experiments. We included the
966 conversion of 100 nM 11KA4 to 11OHA4 in all experiments and used the initial rate to normalise the transfection
967 efficiency, which was set to 1 for the values reported above.
968 #V_{max}/K_m values are reported for the substrate and forward reaction.